

# Northumbria Research Link

Citation: Wang, Caiyun, Xu, Bin, Zhang, Xuan, Sun, Wenping, Chen, Jian, Pan, Hongge, Yan, Mi and Jiang, Yinzhu (2022) Ion Hopping: Design Principles for Strategies to Improve Ionic Conductivity for Inorganic Solid Electrolytes. *Small*, 18 (43). p. 2107064. ISSN 1613-6810

Published by: Wiley-Blackwell

URL: <https://doi.org/10.1002/smll.202107064> <<https://doi.org/10.1002/smll.202107064>>

This version was downloaded from Northumbria Research Link:  
<https://nrl.northumbria.ac.uk/id/eprint/48804/>

Northumbria University has developed Northumbria Research Link (NRL) to enable users to access the University's research output. Copyright © and moral rights for items on NRL are retained by the individual author(s) and/or other copyright owners. Single copies of full items can be reproduced, displayed or performed, and given to third parties in any format or medium for personal research or study, educational, or not-for-profit purposes without prior permission or charge, provided the authors, title and full bibliographic details are given, as well as a hyperlink and/or URL to the original metadata page. The content must not be changed in any way. Full items must not be sold commercially in any format or medium without formal permission of the copyright holder. The full policy is available online: <http://nrl.northumbria.ac.uk/policies.html>

This document may differ from the final, published version of the research and has been made available online in accordance with publisher policies. To read and/or cite from the published version of the research, please visit the publisher's website (a subscription may be required.)



**Northumbria  
University**  
NEWCASTLE



University**Library**

# **Ion Hopping: Design Principles for Strategies to Improve Ionic Conductivity for Inorganic Solid Electrolytes**

*Caiyun Wang, Ben Bin Xu, Xuan Zhang, Wenping Sun, Jian Chen, Hongge Pan, Mi Yan, Yinzhu Jiang\**

C. Wang, Prof. W. Sun, Prof. H. Pan, Prof. M. Yan, Prof. Y. Jiang

School of Materials Science and Engineering, State Key Laboratory of Clean Energy Utilization,  
Zhejiang University, Hangzhou 310027, China.

E-mail: [yzjiang@zju.edu.cn](mailto:yzjiang@zju.edu.cn)

C. Wang, Prof. X. Zhang, Prof. Y. Jiang

ZJU-Hangzhou Global Scientific and Technological Innovation Centre, Zhejiang University,  
Hangzhou 311200, P.R. China

Prof. J. Chen, Prof. H. Pan

Institute of Science and Technology for New Energy, Xi'an Technological University, Xi'an  
710021, P.R. China

Prof. B. B. Xu

Mechanical and Construction Engineering, Faculty of Engineering and Environment,  
Northumbria University, Newcastle upon Tyne NE1 8ST, UK

**Keywords:** ion hopping, solid electrolytes, batteries, ionic conductivity, ion transport mechanism

**Abstract:**

Solid electrolyte has been considered as an ideal substitution of liquid electrolyte, by avoiding the potential hazards of volatilization, flammability and explosion for liquid electrolyte based rechargeable batteries. However, there are significant performance gaps to be bridged between solid electrolytes with liquid electrolytes, one with the particular importance is the ionic conductivity which is highly dependent on the material types and structures. In this review, we re-visit the general physical image of ion hopping in the crystalline structure, by highlighting two main kernels that impact ion migration: ion hopping pathways and skeletons interaction. We then systematically summarize the universal strategies to effectively improve ionic conductivity of inorganic solid electrolytes: (1) constructing rapid diffusion pathways for mobile ions; (2) reducing resistance of the surrounding potential field. The scoped strategies offer an exclusive view on the working principle of ions movements regardless of the ion species, thus providing a comprehensive guidance for the future exploitation of solid electrolytes.

## 1. Introduction

The concerns over global climate change, accelerated by the consumption of fossil fuels and increasing CO<sub>2</sub> emissions, have stimulated explosive researches on renewable energy technologies with clean and sustainable sources.<sup>[1-3]</sup> From this perspective, the energy storage systems with green energy sources (solar, wind, tidal) are under urgent demand to compensate their intermittent characteristics.<sup>[4]</sup> Rechargeable batteries, proven to be an efficient and environment-friendly energy storage technology, have sparked massive research enthusiasms.<sup>[5]</sup> Benefiting from the high energy density and long cycling lifetime, lithium ion batteries (LIBs) have created a remarkable commercial success, by powering products from portable electronics to electric vehicles.<sup>[6-8]</sup> On the other side, there are increasing health and safety cases reported, regarding to the fire and exploding incidents of using batteries.<sup>[9, 10]</sup> One of the latest research trends focus on exploring alternative electrolyte systems to mitigate the safety dilemma caused by the flammable liquid nature of traditional liquid electrolyte.<sup>[11]</sup>

Solid electrolyte has been considered as an ideal substitution of the current liquid electrolyte as their unique characteristics: (1) Solid electrolytes with un-flammable nature can fundamentally avoid the fire danger and electrolytes leakage, providing as the essential component for more secure battery systems. (2) The use of solid electrolytes can be expected with higher energy density and longer cycling lifetime, as they generally accompanied by high chemical stability, which makes it possible to investigate cathodes with high voltage and directly use metal anode. (3) The undesirable side reaction, occurring in liquid electrolytes battery systems, can be effectively restrained. For instance, the ubiquitous shuttle effect in metal-sulfur batteries with liquid electrolytes will seriously damage the coulombic efficiency and cycling lifetime, which can be greatly suppressed by using solid electrolytes as the polysulfide cannot migrate. (4) Solid electrolytes possess superiority in practical operation, with a wider operating temperature and electrochemical stability window to tolerate the complex working conditions.<sup>[12]</sup> As the crucial part in solid-state battery, solid electrolyte needs to

achieve extraordinary performance with high ionic conductivity, wide electrochemical window, tight and stable contacted interface between electrolyte and electrodes, and good mechanical and thermal stability.

According to the composition, the reported solid electrolytes can be classified as solid polymer electrolytes,<sup>[13]</sup> inorganic solid electrolytes,<sup>[14]</sup> and composite electrolytes<sup>[15, 16]</sup>, exhibiting different superiority. Polymer electrolytes with flexible character can provide well-contacted interface between electrolyte and electrodes for effectively ion transport. However, the intrinsic low ionic conductivity confines the usage of flexible polymer electrolytes, which can be enhanced by inorganic filler additives. Inorganic solid electrolytes usually have fast ion transport with high thermal stability, appearing high ionic conductivity. Whereas, the poor interfacial contact of electrolyte and electrodes extremely damage the battery performance. To address this issue, many methods have been reported to improve the interface contact. Ceramic/polymer composite electrolytes are believed to combine the advantages of these two types of solid electrolytes, getting some progress. Even though, there is no perfection that can reach all the requirements for battery use currently. Selecting an appropriate solid electrolyte with high ionic conductivity is still urgent and the prerequisite for solid-state battery system design, thus emphasizing exploration of inorganic ionic conductors.

Nowadays, a plenty of inorganic ionic conductors for various mobile metal ions, including  $\text{Li}^+$ ,<sup>[17]</sup>  $\text{Na}^+$ ,<sup>[18]</sup>  $\text{Mg}^{2+}$ ,<sup>[19, 20]</sup>  $\text{Zn}^{2+}$ ,<sup>[21, 22]</sup> etc, have been exercised for solid state batteries.<sup>[23]</sup> Sulfide solid electrolytes, such as  $\text{Li}_3\text{PS}_4$ ,  $\text{Li}_2\text{S}-\text{P}_2\text{S}_5$ ,  $\text{Li}_{10}\text{GeP}_2\text{S}_{12}$  (LGPS), appear to be a promising solid electrolyte candidates for solid-state lithium batteries, appending high ionic conductivity about  $10^{-2}$  S cm<sup>-1</sup>.<sup>[24]</sup> Garnet-type oxides, such as  $\text{Li}_7\text{La}_3\text{Zr}_2\text{O}_{12}$  (LLZO),<sup>[25]</sup> NaSICON-type  $\text{Li}_{1+x}\text{Al}_x\text{Ti}_{2-x}(\text{PO}_4)_3$  (LATP) and  $\text{Li}_{1+x}\text{Al}_x\text{Ge}_{2-x}(\text{PO}_4)_3$  (LAGP),<sup>[26]</sup> are another competitors for solid electrolytes with unique Li-ion conductivity of  $10^{-4}$ - $10^{-2}$  S cm<sup>-1</sup>. NaSICON-type oxides can also be used as solid electrolytes, typically  $\text{Na}_3\text{Zr}_2\text{Si}_2\text{PO}_{12}$  (ionic

conductivity:  $10^{-3}$ – $10^{-2}$  S cm $^{-1}$ ).<sup>[27]</sup> Recently, MgSc<sub>2</sub>Se<sub>4</sub> was also reported as a potential solid electrolyte in magnesium batteries with an ionic conductivity of  $10^{-4}$  S cm $^{-1}$ .<sup>[28]</sup>

As an essential criterion, a high ionic conductivity equivalent to the level of traditional liquid electrolyte ( $>10^{-2}$  S cm $^{-1}$ ) is desired for solid electrolytes. Unfortunately, though vast painstaking efforts are devoted to hunting for satisfied solid electrolytes, considerable gaps remain to be bridged to reach favoured ionic conductivity. The primary gap is the lack of new/novel ion transporting mechanism to enhance the ionic conductivity, where insightful scientific understandings on the ionic conduction in solid conductors appears as a critical element to exploit remarkable solid electrolytes. The generally accepted fundamental microcosmic physical image of ion migration in ionic conductors is that the mobile ions jump from one occupied position to another.<sup>[29]</sup> Up to now, there are multitudes of reviews to elaborate different ion transport mechanisms of various existing solid electrolytes.<sup>[30, 31]</sup> However, the universal roadmap for enhancing ionic conductivity remains yet to be charted.

In this article, we holistically summarize the strategies to improve ionic conductivity, through investigating ion hopping process to reveal the general influencing factors in ionic conduction, not confined on one specific mobile ion. The conduction of metal ions in inorganic solid electrolyte can be simplified as directional hopping of mobile ions, clarified as jump relaxation model.<sup>[32]</sup> The hopping of the ions is intrinsic thermally driven, where diffusion path in the crystal structure is crucial. Meanwhile, the tight interactions of skeletons with mobile ions block the ion movements, then affecting ionic conductivity. Therefore, the fundamental concepts in enhancing ionic conductivity can be classified as: (1) constructing rapid diffusion pathways for mobile ions; (2) reducing resistance of the surrounding potential field (**Figure 1**). In line with above classifications, the possible directions and approaches are summarized to enable further solid electrolytes, to develop future all-solid-state batteries with bespoken performance.

## 2. Fundamentals for Ion Migration

Many materials can be potentially used as fast ionic conductors for different mobile metal ions. Although multifarious ion migration models are proposed to describe the microcosmic process, they share the basic physic principles.<sup>[33]</sup> Commonly the mobile ions in crystalline solids tend to occupy the lowest energy sites, whose migration process can be regarded as a continuous hopping of ions at these locations.<sup>[34]</sup> When the displacement is R after jumping n times, the diffusion coefficient (D), which measures the hopping rate of ions in the structure, can be expressed as:

$$D = \frac{\langle R^2 \rangle}{bt} = \frac{1}{b} vr^2 \quad (1)$$

where t is lasting time of n jumps, v is the jump frequency, r is the distance of one jump and b represents the geometrical factor. From **Equation 2**, also called Nernst-Einstein equation, the ionic conductivity  $\sigma$  is proportional to the diffusion coefficient D:

$$\sigma = \frac{Dnq^2}{kT} \quad (2)$$

where n is the number of mobile ions per unit volume, q is the quantity of electric charge of one mobile ion. For solid electrolyte materials, large diffusion coefficient (D) and high ionic conductivity ( $\sigma$ ) are both required. In crystalline structures, mobile ions generally migrate through point defects (**Figure 2a**). Take vacancies as an example, where the diffusion of ions can be equivalent to the diffusion of vacancies. Here comes the equation:

$$D_v C_v = DC \quad (3)$$

where  $D_v$  is diffusion coefficient of vacancies,  $C_v$  is concentration of vacancies, D is diffusion coefficient of mobile ions, and C is concentration of mobile ions. Since the generation of vacancies is a process of thermal excitation:

$$C_v = C_{v0} \exp\left(-\frac{E_v}{RT}\right) \quad (4)$$

where  $E_v$  is formation energy of vacancies. When the concentration of mobile ions in a solid is dilute enough, which means the ions jumps are independent, the movement of ions follows a random thermal-driven Brownian motion. The same goes for vacancies:

$$D_v = \frac{1}{b} v_v r^2 = \frac{1}{b} r^2 v_{v0} \exp\left(-\frac{E_j}{RT}\right) \quad (5)$$

where  $E_j$  is the activation energy for vacancies to jump. Combining **Equations 3-5**, we can obtain:

$$D = \frac{1}{b} r^2 v_{v0} \frac{C_{v0}}{C} \exp\left(-\frac{E_v + E_j}{RT}\right) \quad (6)$$

Hence, the activation energy of ion migration can be determined by  $E_v$  and  $E_j$ . Upon introducing a large quantity of vacancies (defect regulation), the ionic conductivity can be obviously enhanced in terms of the constant of  $C_v$  and the neglected  $E_v$ . In fact, the ions can jump in a variety of ways. The activation energy is variable depending on how ions jump, leading to the difference in  $E_v$ . Thus, a rapid hopping path for ions is crucial for accelerating ion migration. On the other hand, the opposite charged skeleton attracts mobile ions in the consideration of electric neutrality. When ions jumping, this Coulomb force need to be overcome, reflecting in  $E_j$ . From this perspective, the reduction of interaction between mobile ions and the skeleton seems to be a feasible route. Figure 2b-d<sup>[32]</sup> depicts the hopping of charged ions in the periodic potential field. The potential energy is a function related to migration distance of mobile ions, where the lowest energy represents the equilibrium position and the highest energy represents the position closest to anions, determining the barrier for migration. Regulating  $E_v$  means finding a new migration path with gentle energy fluctuation, while controlling  $E_j$  means reducing the highest energy position for the specific migration path, both lowering the barrier for ion migration, having irreplaceable significance for enhancing ionic conductivity.

Notably, we assume a general mobile ion in the model, without consideration of valence or radius of the ions, which could be applied to most ions. While, situations may be slightly

different for various ions. Li-ion conductors have been extensively explored as their great commercial potential.  $\text{Na}^+$  has the same valence of  $\text{Li}^+$ , making many similarities of these two categories. For instance, NaSICON-type materials have been verified as available solid electrolytes for both solid-state lithium and sodium batteries. Whereas,  $\text{Na}^+$  has larger ionic radius, requiring larger conduction channels in the materials. As for multivalent metal-ions, the researches of solid electrolytes are rare as the large migration barrier caused by the increasing charge and volume.

### **3. Constructing Rapid Diffusion Pathways for Mobile Ions**

The activation energy and ionic conductivity of solid electrolytes has a strong correlation with the diffusion pathway, which is determined by the crystalline structure, auxiliary defects and ions. In this section, we discuss strategies for enhancing ionic conductivity by constructing rapid diffusion pathways.

#### **3.1. Crystalline Structure for Ion Migration**

Empirically, a satisfactory structure for guaranteeing rapid ion migration needs to attain some requirements.<sup>[35]</sup> In the certain crystalline structure, the mobile ions prefer locating the stable sites with the lowest energy, the ion hopping between these sites leading ionic conduction.<sup>[36]</sup> Accordingly, a continuous hopping of mobile ions in a long enough range is pre-requisite for observable ionic conductivity, which requires the connected channels between adjacent sites in long-range ordered structure. The connected conduction channels should possess appropriate size, allowing the rapid movement of mobile ions. Moreover, the different sites of mobile ions along the channels need to keep a relative flat energy landscape, maintaining a low migration barrier. From this perspective, when the randomly distributed mobile ions across the conduction channels are favorable for the improvement of ionic conductivity.

Ceder *et al.* proposed design principles for solid-state lithium superionic conductors and revealed the critical influences of the anion-host matrix on the ionic conductivity of solid-state

Li-ion conductors.<sup>[37]</sup> The results indicated that body-centered cubic (bcc) anion framework allows the Li ions to migrate within a network of interconnected tetrahedral sites possessing equivalent energies, yielding a lower activation barrier (**Figure 3a**) as verified in  $\text{Li}_{10}\text{GeP}_2\text{S}_{12}$  and  $\text{Li}_7\text{P}_3\text{S}_{11}$ . Apart from ionic conductors with 3D diffusion channels, layered structures with 2D-diffusion also show promises as solid electrolytes.<sup>[38]</sup> A new P2-type honeycomb-layered  $\text{Na}_2\text{Mg}_2\text{TeO}_6$ , with  $\text{Na}^+$  migration pathway created in the crystal lattice between two honeycomb frameworks, exhibited a high ionic conductivity of  $2.3 \times 10^{-4} \text{ S cm}^{-1}$  (Figure 3b).<sup>[39]</sup> Recently, a special structure of  $\text{KSi}_2\text{P}_3$  with T5 supertetrahedra was demonstrated for rapid  $\text{K}^+$  migration, where the  $\text{KSi}_2\text{P}_3$  is composed of  $\text{SiP}_4$  tetrahedra forming interpenetrating networks of large T5 supertetrahedra.<sup>[40]</sup> The potassium ions located in large channels between the T5 supertetrahedral networks shows facile movement through the structure (Figure 3c). Emphatically, the best performing structure for various active ions are different, which makes the choice of an applicable crystalline structure essential for rapid ion migration.<sup>[41-44]</sup> The typical structures and materials for solid electrolytes of various active ions are listed as **Table 1**.

### 3.2. Defect Regulation

The perfect periodic structure is almost impossible to obtain experimentally, since crystal solids are always accompanied by various defects, intrinsic and extrinsic.<sup>[58]</sup> It is worth noting that we only discuss the defects which are directly relevant to ion migration pathways, the skeletal defects introduced to regulating the dynamic stability of the crystal framework therefore is deferred.

The mobile ions usually do not completely fill the sites in the fast ionic conductors, existing fraction occupying ratio naturally and leading to many vacancies for ion migration. Recently, Searles *et al.* calculated the vital effect of structural defects and investigated diffusion coefficient of Li ions in  $\text{Li}_3\text{OCl}$ , a typical anti-perovskite Li-ion conductor.<sup>[59]</sup> Anti-perovskite

materials are usually filled with intrinsic defects to maintain the structural stability due to the uniqueness of their structure, making them possess relatively high ionic conductivity. Three kinds of point defects (LiCl Schottky defect, Li<sub>2</sub>O Schottky defect, and O-Cl substitution defect) are likely to occur (**Figure 4a**). The types, distributions, and combinations of defects significantly affect the Nernst–Einstein conductivity and ion diffusion activation energy (**Figure 4b**). Whereas, the intrinsic defects in solids can only be introduced during the synthesis process with uncertainty. Yashima *et al.* reported a hexagonal perovskite related oxide-ion conductors Ba<sub>7</sub>Nb<sub>3.9</sub>Mo<sub>1.1</sub>O<sub>20.05</sub>, containing an excess oxygen of  $x=0.05$  (O<sub>20+x</sub> or O<sub>0.05</sub>) in Ba<sub>7</sub>Nb<sub>3.9</sub>Mo<sub>1.1</sub>O<sub>20.05</sub>) compared with the mother material (Ba<sub>7</sub>Nb<sub>4</sub>MoO<sub>20</sub>).<sup>[60]</sup> The O1–O5 oxide ion interstitially diffusion was striking accelerated by the increased interstitial oxygen, leading a higher oxide-ion conductivity of Ba<sub>7</sub>Nb<sub>3.9</sub>Mo<sub>1.1</sub>O<sub>20.05</sub> (**Figure 4c, d**). In practical scenarios, the intrinsic defects of crystals are tightly related to temperature (**Equation 4**), which are challenging to targeted defect types and concentrations.

Aliovalent ions doping is commonly considered to be a realistic approach to regulate defects in crystalline solids, which is confirmed in plentiful ionic conductors for various mobile ions.<sup>[61, 62]</sup> Element substitution of the active ion site can remarkably influence the vacancy and carrier concentration even with a small number of foreign ions. Theoretically, Huang *et al.* simulated the migration of Na<sup>+</sup> in Ca<sup>2+</sup>-doped Na<sub>3</sub>PS<sub>4</sub>.<sup>[63]</sup> When the doped Ca<sup>2+</sup> replacing the Na II site, Na vacancies are generated to ensure electron neutrality, as depicted in **Figure 4e**. The migration through the path of Na I–Na II–Na I (**Figure 4f**) is accelerated by the introduced Na vacancies, lowering the migration energy barrier (0.21 eV→0.19 eV). Similarly, aliovalent substitution on skeleton site is capable of altering carrier concentration. Ran *et al.* reported a Sc, Ge doped on Zr site for NaSICON type sodium superionic conductor (Na<sub>3.125</sub>Zr<sub>1.75</sub>Sc<sub>0.125</sub>Ge<sub>0.125</sub>Si<sub>2</sub>PO<sub>12</sub>, **Figure 4g**) with increased Na<sup>+</sup> concentration, achieving enhanced ionic conductivity of 4.64  $\times 10^{-3}$  S cm<sup>-1</sup> (**Figure 4h**).<sup>[64]</sup> Besides, doping on skeleton sites can modify the electrostatic

interactions between the mobile Li ions and surrounding framework anions, which is categorized into Section 4.

### 3.3. Concerted Migration

In Section 2, we simplify the classical diffusion model as the independent hopping of individual ions from one lattice site to another, neglecting the correlated migration of multiple ions. To fit the actual situation, the correlation factor  $f$  and Haven ratio  $H_R$  are introduced to evaluate the deviation.<sup>[65]</sup> Here comes the **Equation 7**:

$$D = \frac{f}{H_R} \frac{1}{b} r^2 v_{v0} \frac{C_{v0}}{C} \exp\left(-\frac{E_v + E_j}{RT}\right) \quad (7)$$

The correlation factor  $f$  generally takes a value between 0 and 1, measuring the interrelation of various hopping.<sup>[66]</sup> While  $H_R$  has no specific physical meaning, reflecting the coupling of different migration mechanisms. When  $f=1$ ,  $H_R=1$ , Equation 7 is equivalent to Equation 6, representing that the hopping of ions is individual and random. It has been verified that the migration barrier can be significantly lowered when two or more ions interknit jump.

The so-called “kick-off”,<sup>[67]</sup> “interstitially”<sup>[68]</sup> migration mechanism shares the same principle as the concerted migration for two or more ions involved in the hopping of mobile ions. Notably, concerted migration describes an associated hopping of ions in different chemical environments, remarkably reducing the migration barrier compared with single-ion migration (**Figure 5a**).<sup>[69]</sup> For typical NaSICON materials, three  $\text{Na}^+$  sites (Na1, Na2, Na3) with different energy exist in  $\text{NaZr}_2(\text{PO}_4)_3$ , where Na1 site is a low energy site.<sup>[70]</sup> On the basis of climbing image nudged elastic band (CI-NEB) method, the concerted migration was occurred by  $\text{Na}_2 + \text{Na}_1 + \text{Va}(\text{Na}_2) \rightarrow \text{Va}(\text{Na}_2) + \text{Na}_1 + \text{Na}_2$  with a lowest barrier (Figure 5b). As a result, the  $\text{Na}^+$  ion originally located at the Na2 site moved toward the next Na1 site and the strong Coulomb force pushed that  $\text{Na}^+$  ion to the next Na2 site, achieving the migration barrier of 0.103 eV. The concerted migration is often discovered in materials with high concentration of active ions, where the lowest energy sites are fully filled and extra ions are occupied sites with relatively

high energy. For ion migration, the ions with different energy move simultaneously, the energy difference between these two kinds of ions whittling the barrier. In this mode, the ionic conductivity is often optimized by modulating the carrier concentration, where substituting is still a practical method.<sup>[71, 72]</sup> What's more, the concerted migration can be expanded to the associated hopping involving two different types of mobile ions and/or mobile ions/skeleton ions, which is deserved for further investigation with enhanced ionic conductivity.<sup>[73]</sup> Noteworthily, the concerted migration of two different mobile ions has been reported frequently in the cathode materials, indicating potentials for solid electrolytes.<sup>[74]</sup>

#### 4. Reducing Resistance of Surrounding Potential Field

##### 4.1. Phonon–Ion Interactions

The energy landscape of mobile ions in crystalline lattice depends not only on the crystal structure, but also on the bonding interaction of skeleton ions. Even for the same structure, there considerable discrepancy exists in migration barrier as the results of different skeleton anions.<sup>[75]</sup> Such vital effect of skeleton ions can be seen as the interactions of mobile ions and phonons derived from lattice dynamics.<sup>[76]</sup> The crucial influence of phonons on ionic conductivity was discovered and demonstrated experimentally in Ag-ion conductors since last century.<sup>[77, 78]</sup> Though many theories and models have been proposed to predict a descriptor for measuring the phonon-ion coupling<sup>[77, 79]</sup>, a detailed and appropriate understanding of how lattice dynamic influence the ionic conduction is still absent. Recently, the physical images of lattice dynamics are attracting attention with the potentials for Li-ion conductors of solid-state lithium batteries. Some rules experimentally verified can give some directions.

During the hopping of a mobile ion, the saddle point must be crossed, heavily dependent on the anharmonic relaxational motion from the skeleton lattice (**Figure 6a**).<sup>[80]</sup> Typical terms/concepts associating with the anharmonic potential are summarized as follows:

(1) Lattice polarizability: The polarizability of ions is considered as the ability to form instantaneous dipoles, as determined by the size and charge. For anions that exhibit the same formal charge, the one with larger size is more polarizable.<sup>[81]</sup> In terms of bonding, the polarizability closely relates to the bond strength, where the anions with larger polarizability likely to have wider spread electron cloud distribution and weak bond connection. The lattice of more polarizable anions generally represents the weak phonon-ion interaction and decreasing diffusion barrier (Figure 6b).<sup>[76]</sup>

(2) Debye frequency: Within the framework of the transition state theory of ionic motion, the mobile ions are trapped in a potential well with an energy gap. The attempt frequency is defined as the rate that a bound ion "attempts" to escape the potential, corresponding to the energy barrier.<sup>[82]</sup> The value of attempt frequency is usually within the range of phonon frequency, so it is possible to use Debye frequency as a descriptor to estimate the attempt frequency in certain conditions. The Debye frequency decreases as the lattice becomes softer, leading a decreasing attempt frequency and activation energy (Figure 6c, d).<sup>[83]</sup> It is worth noting that, even the Debye frequency and the attempt frequency seem to have some kind of connections, they are not totally equated to each other. This deviation is originated by the involvement of the optical phonons in the lattice, which Debye frequency neglects the impact.<sup>[84]</sup> As the jumping frequency also appeared in pre-exponential factor of ionic conductivity (Equation 6), the soften lattice is also accompanied by reducing pre-exponential factor and then impairing ionic conductivity, which might be an explanation for Meyer-Neldel rule (or compensation rule).<sup>[85]</sup>

(3) Phonon band center: Phonon band center is a new term in describing the anharmonic potential by comprehensively considering the influence of phonon vibration, which can be measured and calculated via statistically averaging over the vibrational spectrum weighted by the phonon density of states at each frequency.<sup>[86]</sup> Lowering the lithium phonon band center of the Li-sublattice can effectively reduce the enthalpy of migration in different Li-ion conductors (Figure 6e).<sup>[75]</sup> Notably, the phone band center has a correlation with Debye frequency.

Even though these terms/concepts can connect lattice dynamic with ion migration, which are considerable reference factors when searching potential ionic conductors. In some circumstances, these conceptions might be unapplicable and even contradictory, which should be analyzed case by case. However, despite many efforts have been paid to understand possible connections of lattice dynamic on the ion migration processes, no unified theory has been achieved.

#### 4.2. Lattice Softness

The softer, more polarizable anion framework benefit the ionic transportsations, by decreasing Debye frequency and Phonon band center. **Figure 7a** depicts the variation of energy landscape of specific  $\text{Li}^+$  when lattice softening.<sup>[83]</sup> By softening lattice, which means to weaken the bond interaction of mobile ions and skeleton ions, the local jump mode reaches a board oscillation, thereby reduce the activation barrier.<sup>[87]</sup> Anions substitution has been frequently corroborated to soften the lattice framework in  $\text{Li}^+$ - and  $\text{Na}^+$ -conductors. For instance, Se possesses the same formal charge and larger ionic radius comparing with S, making it more polarizable and suitable to construct a softer framework (Figure 7b).<sup>[88, 89]</sup> In line with the above principle, the ionic conductivities of argyrodites  $\text{Li}_6\text{PS}_5\text{X}$  ( $\text{X} = \text{Cl}, \text{Br}$ ) can be optimized by tailoring the anions.<sup>[90]</sup> Actually, there are usually non-mobile cation elements contained in ionic conductors beyond mobile cations and skeleton anions, which also playing an important role in lattice. Feng *et al.* doped Tungsten in sodium thioantimonate, to achieve a lower activation energy.<sup>[91]</sup> The heavy W-doping lower the local Na-S interactions by pulling the S away from Na-ions through the strong W-S interaction, creating a “softer” S and facilitating Na-ion migration (Figure 7c). Xu et al. systematically studied the effects of charge and lattice volume on the stability of lithium ion occupation and migration in face-centered cubic (fcc) structure.<sup>[92]</sup> Low lithium ion migration barriers can be achieved by adjusting the non-lithium elements within the same crystal structure. Figure 7d highlights the recommended element of the skeleton ions in the periodic table of element to achieve fast A ion migration in the ABC ternary compounds.

Tuning the softness of lattice are often accompanied by some distortions of structure and introducing defects in the crystal lattice, further affecting the ionic conductivity.<sup>[93-95]</sup>

However, there are some puzzles remain to be resolved as some experimental results stand oppositely to the idea that a softer lattice framework is beneficial for ionic conduction, for example, the more polarizable Li<sub>3</sub>OB<sub>r</sub> shows a lower ionic conductivity than Li<sub>3</sub>OCl.<sup>[96, 97]</sup> Similarly, Li<sub>6</sub>PS<sub>5</sub>I appears an extraordinary low ionic conductivity compared with Li<sub>6</sub>PS<sub>5</sub>Br and Li<sub>6</sub>PS<sub>5</sub>Cl.<sup>[98]</sup> An empirical rule has been generally utilized to explain the anomalous phenomenon for various ionic conductors, known as Meyer-Neldel rule.<sup>[99]</sup> Whereas, the Meyer-Neldel rule can't be universally applied to all ionic conductors. The decreasing of pre-exponential factor correlating with the reduction of activation barrier can be attributed to the entropy of migration. The multi-excitation entropy theory seems to be a possible explanation to bridge this gap, which describes activation entropy proportional to the activation energy.<sup>[100]</sup>

#### 4.3. Structural Disorder or Distortion

Since the migration entropy has a crucial impact on the ionic conduction, altering the structural disorder or distortion has been proved as an effective approach to enhance ionic conductivity. LiTi<sub>2</sub>(PS<sub>4</sub>)<sub>3</sub>, an anti-Meyer-Neldel rule material, exhibits an extraordinary high Li-ion diffusion coefficient benefiting from low activation energy and a high pre-exponential factor, with a frustrated energy landscape caused by the highly distorted Li sites (**Figure 8a**).<sup>[101]</sup> Recently, Chen *et al.* analyzed the influence of structural distortion on Li<sub>3</sub>OCl<sub>1-x</sub>Br<sub>x</sub> ionic conductors, suggesting that more distorted initial Li sites and less distorted saddle sites assisted in fast ion migration (Figure 8b).<sup>[102]</sup> The flatter energy landscape was particularly fit for lower activation energy and higher migration entropy, enabling the violation of the rule.

Introducing structural disorder can be used to accelerate the ion migration. Li<sub>6</sub>PS<sub>5</sub>I, as a recognized poor ionic conductor with its ordered anion sublattice, can be enhanced by mechanical treatment, to increase the degree of structural disorder and boost ionic conductivity by 2 orders of magnitude.<sup>[103]</sup> Site disorder has been predicted for higher conductivity by

simulations and verified experimentally. Doping Cl at S (4d) site of argyrodites  $\text{Li}_{6-x}\text{PS}_{5-x}\text{Cl}_{1+x}$  leaded a 1S3Cl (4d) configuration, contributing  $\text{Li}^+$  with significantly higher mobility (Figure 8c).<sup>[104]</sup> Furthermore, a special rock-salt (A1B1)-structured solid electrolyte has been reported with structural disorders as the Li, Al, and H atoms occupying the A sites and O and Cl atoms occupying the B sites (Figure 8d).<sup>[105]</sup> The disorder was induced by configurational entropy and the entropy of mixing reduced the ion hopping barrier and promoted the  $\text{Li}^+$  transport. Such mechanism can be used to construct material system with high entropy towards novel solid conductors.

The orientational disorder of lattice has been evidenced with the lower activation barriers. The new argyrodite  $\text{Li}_6\text{PS}_5\text{CN}$  containing orientationally disordered cyanide ions exhibited a relative low lithium ion migration barrier, though it adopting the similar crystal structures with  $\text{Li}_6\text{PS}_5\text{Br}$  (Figure 8e).<sup>[106]</sup> This strategy could be innovatively applied in ionic conductors for multivalent metal-ions. Yan *et al.* predicted  $\text{NH}_3$  in  $\text{Mg}(\text{BH}_4)_2\text{NH}_3$  exchanged and constructing a highly flexible structure, profiting from the di-hydrogen bonds and dramatically improving the Mg-ion conductivity approximately 8 orders of magnitude higher than that of  $\text{Mg}(\text{BH}_4)_2$  (Figure 8f).<sup>[107]</sup> Therefore, the creation of a chaotic structure like some glass solids with topological disordering of atom arrangement and increased entropy could be a potential strategy for enhancing ionic conductivity.

#### 4.4. Paddle Wheel Mechanism of Polyanions

In 1990s, the paddle-wheel mechanism was proposed to explain the “rotor phases” in high temperature of order-disorder transformation.<sup>[108]</sup> The core concept is that the rotational/reorientational motion of polyanions in the structure may reduce the fluctuation of energy and improve cationic conductivity (**Figure 9a**).<sup>[109]</sup> This phenomenon has been investigated in many structures with covalent bonds polyanions (e.g.,  $\text{NO}_2^-$ ,  $\text{PO}_4^{3-}$ ,  $\text{SO}_4^{2-}$ ). In fact, the rotation of polyanions yields a orientational disorder of anion framework, increasing the structural entropy of the lattice. The paddle-wheel mechanism has special universality and

comes into view to manipulate the ion migration. However, the intrinsic connection of fast rotations of polyanions with cation diffusion is still intricate.

Recently, the rotation of polyanions has been observed in many ionic conductors, typically  $\text{Li}_3\text{PS}_4$ , argyrodites  $\text{Li}_6\text{PS}_5\text{X}$  ( $\text{X} = \text{Cl}, \text{Br}, \text{I}$ ),  $\text{Na}_{11}\text{Sn}_2\text{PS}_{12}$  and so on. For instance,  $\text{Li}_3\text{PS}_4$  exists two type of structures with high-temperature (HT)  $\beta$ -phases and stable low-temperature (LT)  $\gamma$ -phase, appearing ionic conductivity with significant discrepancy.<sup>[109]</sup> The polyanions in two modifications were explored to be arranged differently, determining the divergence of ionic conductivity. In  $\gamma\text{-Li}_3\text{PS}_4$ , the  $[\text{PS}_4]$  tetrahedra feature a  $\text{T}^+$  arrangement along the  $\text{c}$  axis, while the  $[\text{PS}_4]$  tetrahedral arrangement is disordered in  $\beta\text{-Li}_3\text{PS}_4$  (Figure 9b). Whereas the particular disorder arrangement of  $[\text{PS}_4]$  tetrahedral only occur in HT-phase, seeking an approach to maintain the disorder structure in room temperature is required. Zhang *et al.* tuned anion rotation at room temperature by partially substituting  $\text{P}^{5+}$  in  $\text{Li}_3\text{PS}_4$  with  $\text{Si}^{4+}$ , where the Si-substituted analog exhibited an anionic framework with rapid  $[\text{PS}_4]$  rotation, thus lowering the energy barrier for ion migration.<sup>[109]</sup> Smith *et al.* predicted a glass  $75\text{Li}_2\text{S}-25\text{P}_2\text{S}_5$  solid with a long-range disorder covalent network and Li mobility was enhanced by paddlewheel effect of  $\text{PS}_4^{3-}$  tetrahedra.<sup>[110]</sup> Besides, the dynamic of rotation depends extremely on the type of anion. Zhang *et al.* demonstrated the greatly hindered  $[\text{SbS}_4]^{3-}$  rotation compared with  $[\text{PS}_4]^{3-}$  in  $\text{Na}_{11}\text{Sn}_2\text{PnX}_{12}$  ( $\text{Pn} = \text{P, Sb}; \text{X} = \text{S, Se}$ ).<sup>[111]</sup> The variable temperature neutron diffraction/MEM analysis indicated that fast  $[\text{PS}_4]$  rotation is correlated with higher  $\text{Na}^+$ -ion conductivity, whereas the  $[\text{SbS}_4]^{3-}$  exhibited a negligible rotational dynamic even in high temperature. This cation-anion dynamic coupling was though transient widening of the bottleneck for cation migration when anion rotation (Figure 9c, d). Despite above progresses, a deep-going physical model needs to be proposed to reveal the intricacy interaction of anion rotation and cation migration, and a general principle for the choice of anions type need be explored to guide the design of ionic conductor.

## 5. Conclusions and Future Perspectives

In this review, a periscope summary of strategies to enhance ionic conductivity in ionic conductors is provided based on the classical jump relaxation model and two main approaches are followed: constructing rapid diffusion pathways and reducing resistance of the surrounding potential field. These strategies derived from the principle have been verified to be highly effective, as **Table 2** summarizing typical reports about different strategies and comparing the ionic conductivities. For a certain crystalline structure with connected conduction channels for rapid ionic diffusion, defect regulation is most often used to optimize ionic conductivity as it is convenient and effective by changing the raw material ratio or doping other elements. However, the enhancement of ionic conductivity is limited by the confined defect concentration to maintain the crystalline structure. The application of concerted migration mechanism in solid electrolytes can greatly improve the performance, increasing ionic conductivity by 3-5 orders of magnitude. The emphasis is on design and synthesis of materials with concerted migration mechanism. What's more, searching materials with concerted migration, expanded to the associated hopping involving two different types of mobile ions and/or mobile ions/skeleton ions, is deserved for further investigation with enhanced ionic conductivity. Meanwhile, increasing the lattice softness, usually achieved by doping softer elements, exhibit great potential for reducing the migration energy barrier. Whereas, this rule is not always valid in all cases, which needs combine the consideration of entropy for the systems. Here comes the structural disorder or distortion, significantly influencing the ionic conductivity. Paddle wheel effect of polyanions, as a particular phenomenon discovered in some specific materials, can lead to an extremely disorder in the material, assisting the performance of solid electrolytes. In addition, the establishment and verification of novel ion migration mechanisms are also crucial, requiring the comprehensive understanding of ionic behavior in crystalline solid and advanced characterization.

Despite the outstanding progress has been achieved so far, challenges and opportunities remain as follows:

(1) The optimal crystalline structure for ion migration need to be identified. For various active ions, they have diverse feature and require different crystalline structure. Though a large number of models have been proposed to describe the migration of mobile ions in crystalline structure, the consequence still shows a departure from the experimental situation. How can we predict the structure of ideal ionic conductors? The universal and detailed model is required to establish connections between ion characters and movement. The first principles calculations can be used.

(2) Defects, as the auxiliaries for ion hopping, are vital in solid electrolytes. The type, location and concentration extremely effect the migration of ions. Finding the regularity and interaction both theoretically and experimentally between defects and mobile ions are crucial for designed and directional enhancement of ionic conductors.

(3) Concerted migration with other forms of two different types of mobile ions and/or mobile ions/skeleton ions possesses huge potential for investigation. As reported, concerted migration mechanism exhibits extraordinary improvement of ionic conductivity by 3-5 orders of magnitude. Exploiting materials with concerted migration can greatly expand the available ionic conductors.

(4) A apropos model and descriptor for measuring the correlation of lattice dynamic and ion migration requires proposed. As increasing attentions are paid to the interested impact of phonons interaction on ionic conductivity, we will identify the specific phonons and lattice vibration decided ion migration once a thorough understanding is affirmed, making it possible to select and design specific skeleton frameworks for rapid ion transport.

(5) The entropy of the material has proved to be crucial for ionic conductivity. We believed that searching anti-Meyer-Neldel rule materials with highly distorted structure will be a field

of great potential. Recently, many researches are focused on the extraordinary performance of ionic conductors with the deepgoing comprehending about the reasons for Meyer-Neldel rule lacked. It is essential for the exploitation of novel materials for potential solid electrolytes.

(6) Lots of hindrance for practical application need to be emphasized. Gaining an excellent ionic conductor with high enough ionic conductivity is the first step for achieving solid state battery systems with high safety. The physical and mechanical character determines the manufacturing environment for battery assembly, while the interfaces of anode/electrolyte and cathode/electrolyte is a tough problem as well. For application, more parameters need to be optimized, such as energy density, power density and cycle life.<sup>[114-116]</sup>

In this review, we summarise the ion hopping process of ionic conductors and the strategies for enhancing ionic conductivity, hoping to probe a general approach for accelerating migration of various ions. We expect this review to guidance the ion migration of the lattice and induce some innovative ideas for designing a novel type of solid electrolytes.

### Acknowledgements

This work was supported by the National Key Research and Development Program (2019YFE0111200), the National Natural Science Foundation of China (51722105), Zhejiang Provincial Natural Science Foundation of China (LR18B030001) and the Fundamental Research Funds for the Central Universities (2021FZZX001-09).

Received: ((will be filled in by the editorial staff))

Revised: ((will be filled in by the editorial staff))

Published online: ((will be filled in by the editorial staff))

## References:

- [1] M. Höök, X. Tang, *Energ. Policy* **2013**, *52*, 797.
- [2] D. Shindell, C. J. Smith, *Nature* **2019**, *573*, 408.
- [3] C. Le Quéré, G. P. Peters, P. Friedlingstein, R. M. Andrew, J. G. Canadell, S. J. Davis, R. B. Jackson, M. W. Jones, *Nat. Clim. Change* **2021**, *11*, 197.
- [4] P. D. Lund, *Energy* **2010**, *35*, 647.
- [5] P. Poizot, F. Dolhem, *Energ. Environ. Sci.* **2011**, *4*, 2003.
- [6] N. Nitta, F. Wu, J. T. Lee, G. Yushin, *Mater. Today* **2015**, *18*, 5.
- [7] H. Ali, H. A. Khan, M. G. Pecht, *Journal of Energy Storage* **2021**, *40*, 102690.
- [8] P. Poizot, F. Dolhem, *Energ. Environ. Sci.* **2011**, *4*, 3287.
- [9] P. V. Chombo, Y. Laoonual, *J. Power Sources* **2020**, *478*, 228649.
- [10] L. Kong, C. Li, J. Jiang, M. Pecht, *Energies* **2018**, *11*, 2191.
- [11] R. Chen, W. Qu, X. Guo, L. Li, F. Wu, *Mater. Horiz.* **2016**, *3*, 487.
- [12] A. Manthiram, X. Yu, S. Wang, *Nat. Rev. Mater.* **2017**, *2*, 16103.
- [13] Q. Zhang, K. Liu, F. Ding, X. Liu, *Nano Research*, **2017**, *10*, 4139.
- [14] Z. Gao, H. Sun, L. Fu, F. Ye, Y. Zhang, W. Luo, Y. Huang, *Adv. Mater.* **2018**, *30*, 1705702.
- [15] M. Dirican, C. Yan, P. Zhu, X. Zhang, *Mater. Sci. Eng., R*, **2019**, *136*, 27.
- [16] L. Li, Y. Deng, G. Chen, *J. Energy Chem.* **2020**, *50*, 154.
- [17] F. Zheng, M. Kotobuki, S. Song, M. O. Lai, L. Lu, *J. Power Sources* **2018**, *389*, 198.
- [18] C. Zhao, L. Liu, X. Qi, Y. Lu, F. Wu, J. Zhao, Y. Yu, Y. Hu, L. Chen, *Adv. Energy Mater.* **2018**, *8*, 1703012.
- [19] Z. Liang, C. Ban, *Angew. Chem., Int. Ed.* **2021**, *60*, 11036.
- [20] Y. Zhan, W. Zhang, B. Lei, H. Liu, W. Li, *Front. Chem.* **2020**, *8*, 123.
- [21] P. Yu, Y. Zeng, H. Zhang, M. Yu, Y. Tong, X. Lu, *Small* **2019**, *15*, 1804760.
- [22] X. Zeng, J. Mao, J. Hao, J. Liu, S. Liu, Z. Wang, Y. Wang, S. Zhang, T. Zheng, J. Liu, P. Rao, Z. Guo, *Adv. Mater.* **2021**, *33*, 2007416.

- [23] J. G. Kim, B. Son, S. Mukherjee, N. Schuppert, A. Bates, O. Kwon, M. J. Choi, H. Y. Chung, S. Park, *J. Power Sources* **2015**, *282*, 299.
- [24] Z. Ma, H. Xue, S. Guo, *J. Mater. Sci.* **2018**, *53*, 3927.
- [25] V. Thangadurai, S. Narayanan, D. Pinzaru, *Chem. Soc. Rev.* **2014**, *43*, 4714.
- [26] M. Hou, F. Liang, K. Chen, Y. Dai, D. Xue, *Nanotechnology* **2020**, *31*, 132003.
- [27] N. Anantharamulu, K. Koteswara Rao, G. Rambabu, B. Vijaya Kumar, V. Radha, M. Vithal, *J. Mater. Sci.* **2011**, *46*, 2821.
- [28] L. P. Wang, Z. Zhao Karger, F. Klein, J. Chable, T. Braun, A. R. Schür, C. R. Wang, Y. G. Guo, M. Fichtner, *ChemSusChem* **2019**, *12*, 2286.
- [29] A. T. Fromhold, A.-B. Chen, *Phys. Status Solidi B* **1978**, *90*, 1.
- [30] C. R. A. Catlow, *J. Chem. Soc. Faraday Trans.* **1990**, *86*, 1167.
- [31] J. C. Bachman, S. Muy, A. Grimaud, H. Chang, N. Pour, S. F. Lux, O. Paschos, F. Maglia, S. Lupart, P. Lamp, L. Giordano, Y. Shao-Horn, *Chem. Rev.* **2016**, *116*, 140.
- [32] K. Funke, *Prog. Solid St Chem.* **1993**, *22*, 111.
- [33] C.R.A. Catlow, *Solid State Ionics* **1983**, *8*, 87.
- [34] Y. Gao, A. M. Nolan, P. Du, Y. Wu, C. Yang, Q. Chen, Y. Mo, S. Bo, *Chem. Rev.* **2020**, *120*, 5954.
- [35] Z. Zhang, Y. Shao, B. Lotsch, Y. Hu, H. Li, J. Janek, L. F. Nazar, C. Nan, J. Maier, M. Armand, L. Chen, *Energ. Environ. Sci.* **2018**, *11*, 1945.
- [36] X. He, Q. Bai, Y. Liu, A. M. Nolan, C. Ling, Y. Mo, *Adv. Energy Mater.* **2019**, *9*, 1902078.
- [37] Y. Wang, W. D. Richards, S. P. Ong, L. J. Miara, J. C. Kim, Y. Mo, G. Ceder, *Nat. Mater.* **2015**, *14*, 1026.
- [38] M. A. Evstigneeva, V. B. Nalbandyan, A. A. Petrenko, B. S. Medvedev, A. A. Kataev, *Chem. Mater.* **2011**, *23*, 1174.
- [39] Y. Li, Z. Deng, J. Peng, J. Gu, E. Chen, Y. Yu, J. Wu, X. Li, J. Luo, Y. Huang, Y. Xu, Z. Gao, C. Fang, J. Zhu, Q. Li, J. Han, Y. Huang, *ACS Appl. Mater. Inter.* **2018**, *10*, 15760.

- [40] A. Haffner, A. K. Hatz, O. E. O. Zeman, C. Hoch, B. V. Lotsch, D. Johrendt, *Angew. Chem., Int. Ed.* **2021**, *60*, 13641.
- [41] A. Haffner, A. K. Hatz, I. Moudrakovski, B. V. Lotsch, D. Johrendt, *Angew. Chem., Int. Ed.* **2018**, *57*, 6155.
- [42] T. M. F. Restle, C. Sedlmeier, H. Kirchhain, W. Klein, G. Raudaschl-Sieber, L. van Wüllen, T. F. Fässler, *Chem. Mater.* **2021**, *33*, 2957.
- [43] Z. Zhang, E. Ramos, F. Lalère, A. Assoud, K. Kaup, P. Hartman, L. F. Nazar, *Energ. Environ. Sci.* **2018**, *11*, 87.
- [44] Z. Zou, N. Ma, A. Wang, Y. Ran, T. Song, B. He, A. Ye, P. Mi, L. Zhang, H. Zhou, Y. Jiao, J. Liu, D. Wang, Y. Li, M. Avdeev, S. Shi, *Adv. Funct. Mater.* **2021**, *31*, 2107747.
- [45] Y. Inaguma, M. Nakashima, *J. Power Sources*, **2013**, *228*, 250.
- [46] R. Mouta, M. Á. B. Melo, E. M. Diniz, C. W. A. Paschoal, *Chem. Mater.* **2014**, *26*, 7137.
- [47] L. Xu, J. Li, W. Deng, H. Shuai, S. Li, Z. Xu, J. Li, H. Hou, H. Peng, G. Zou, X. Ji, *Adv. Energy Mater.* **2021**, *11*, 2000648.
- [48] Y. Seino, T. Ota, K. Takada, A. Hayashi, M. Tatsumisago, *Energy Environ. Sci.* **2014**, *7*, 627.
- [49] Y. Kato, S. Hori, R. Kanno, *Adv. Energy Mater.* **2020**, *10*, 2002153.
- [50] R. DeWees, H. Wang, *ChemSusChem* **2019**, *12*, 3713.
- [51] G. Chen, J. Lu, X. Zhou, L. Chen, X. Jiang, *Ceram. Int.* **2016**, *42*, 16055.
- [52] Y. B. Rao, K. K. Bharathi, L.N. Patro, *Solid State Ionics* **2021**, *366*, 115671.
- [53] H. Jia, L. Peng, C. Yu, L. Dong, S. Cheng, J. Xie, *J. Mater. Chem. A* **2021**, *9*, 5134.
- [54] G. V. Nechaevz, E. I. Burmakin, *Russ. J. Electrochem.* **2011**, *47*, 457.
- [55] E. I. Burmakin, G. S. Shekhtman, *Russ. J. Electrochem.* **2005**, *41*, 1501.
- [56] W. Lee, S. Tamura, N. Imanaka, *Chem. Lett.* **2017**, *46*, 1486.
- [57] T. Nestler, S. Fedotov, T. Leisegang, D. C. Meyer, *Crit. Rev. Solid State Mater. Sci.* **2019**, *44*, 298.

- [58] C. R. A. Catlow, *Mater. Sci. Eng.* **1992**, *23*, 375.
- [59] A. Baktash, B. Demir, Q. Yuan, D. J. Searles, *Energy Storage Materials* **2021**, *41*, 614.
- [60] M. Yashima, T. Tsujiguchi, Y. Sakuda, Y. Yasui, Y. Zhou, K. Fujii, S. Torii, T. Kamiyama, S. J. Skinner, *Nat. Commun.* **2021**, *12*, 556.
- [61] D. Butts, J. Schoiber, C. Choi, G. J. Redhammer, N. Hüsing, S. Donne, B. Dunn, *Chem. Mater.* **2021**, *33*, 6136.
- [62] D. Jardón-álvarez, N. Kahn, L. Houben, M. Leskes, *J. Phys. Chem. Lett.* **2021**, *12*, 2964.
- [63] B. Huang, J. Zhang, Y. Shi, X. Lu, J. Zhang, B. Chen, J. Zhou, R. Cai, *Phys. Chem. Chem. Phys.* **2020**, *22*, 19816.
- [64] L. Ran, A. Baktash, M. Li, Y. Yin, B. Demir, T. Lin, M. Li, M. Rana, I. Gentle, L. Wang, D. J. Searles, R. Knibbe, *Energy Stor. Mater.* **2021**, *40*, 282.
- [65] G.E. Murch, *Solid State Ionics* **1982**, *7*, 177.
- [66] R. J. Friauf, *J. Appl. Phys.* **1962**, *33*, 494.
- [67] X. Wang, R. Xiao, H. Li, L. Chen, *Phys. Rev. Lett.* **2017**, *118*, 195901.
- [68] K. Mori, A. Mineshige, T. Saito, M. Sugiura, Y. Ishikawa, F. Fujisaki, K. Namba, T. Kamiyama, T. Otomo, T. Abe, T. Fukunaga, *ACS Appl. Energy Mater.* **2020**, *3*, 2873.
- [69] X. He, Y. Zhu, Y. Mo, *Nat. Commun.* **2017**, *8*, 15893.
- [70] Z. Zou, N. Ma, A. Wang, Y. Ran, T. Song, Y. Jiao, J. Liu, H. Zhou, W. Shi, B. He, D. Wang, Y. Li, M. Avdeev, S. Shi, *Adv. Energy Mater.* **2020**, *10*, 2001486.
- [71] Y. Lee, J. Jeong, H. Lim, S. Kim, H. Jung, K. Y. Chung, S. Yu, *ACS Sustain. Chem. Eng.* **2021**, *9*, 120.
- [72] T. Yajima, Y. Hinuma, S. Hori, R. Iwasaki, R. Kanno, T. Ohhara, A. Nakao, K. Munakata, Z. Hiroi, *J. Mater. Chem. A* **2021**, *9*, 11278.
- [73] P. Hu, Z. Zou, X. Sun, D. Wang, J. Ma, Q. Kong, D. Xiao, L. Gu, X. Zhou, J. Zhao, S. Dong, B. He, M. Avdeev, S. Shi, G. Cui, L. Chen, *Adv. Mater.* **2020**, *32*, 1907526.
- [74] J. Peng, Y. Liu, Y. Pan, J. Wu, Y. Su, Y. Guo, X. Wu, C. Wu, Y. Xie, *J. Am. Chem. Soc.*

**2020**, *142*, 18645.

- [75] S. Muy, J. C. Bachman, L. Giordano, H. Chang, D. L. Abernathy, D. Bansal, O. Delaire, S. Hori, R. Kanno, F. Maglia, S. Lupart, P. Lamp, Y. Shao-Horn, *Energ. Environ. Sci.* **2018**, *11*, 850.
- [76] S. Muy, R. Schlem, Y. Shao Horn, W. G. Zeier, *Adv. Energy Mater.* **2021**, *11*, 2002787.
- [77] K. Wakamura, K. Hirokawa, K. Orita, *J. Phys. Chem. Solids* **1996**, *57*, 75.
- [78] J. Ding, J. L. Niedziela, D. Bansal, J. Wang, X. He, A. F. May, G. Ehlers, D. L. Abernathy, A. Said, A. Alatas, Y. Ren, G. Arya, O. Delaire, *Proc. Natl. Acad. Sci.* **2020**, *117*, 3930.
- [79] T. Tomoyose, *J. Phys. Soc. Jpn.* **1991**, *60*, 1263.
- [80] T. M. Brenner, C. Gehrmann, R. Korobko, T. Livneh, D. A. Egger, O. Yaffe, *Phys. Rev. Mater.* **2020**, *4*, 115402.
- [81] T. Krauskopf, S. Muy, S. P. Culver, S. Ohno, O. Delaire, Y. Shao-Horn, W. G. Zeier, *J. Am. Chem. Soc.* **2018**, *140*, 14464.
- [82] M. J. Rice, W. L. Roth, *J. Solid State Chem.* **1972**, *4*, 294.
- [83] M. A. Kraft, S. P. Culver, M. Calderon, F. Böcher, T. Krauskopf, A. Senyshyn, C. Dietrich, A. Zevalkink, J. Janek, W. G. Zeier, *J. Am. Chem. Soc.* **2017**, *139*, 10909.
- [84] K. Wakamura, *Phys. Rev. B* **1997**, *56*, 11593.
- [85] W. Wieczorek, *Solid State Ionics* **1992**, *53*, 1064.
- [86] S. Muy, J. Voss, R. Schlem, R. Koerver, S. J. Sedlmaier, F. Maglia, P. Lamp, W. G. Zeier, Y. Shao-Horn, *iScience* **2019**, *16*, 270.
- [87] R. Schlem, T. Bernges, C. Li, M. A. Kraft, N. Minafra, W. G. Zeier, *ACS Appl. Energy Mater.* **2020**, *3*, 3684.
- [88] R. Schlem, M. Ghidiu, S. P. Culver, A. Hansen, W. G. Zeier, *ACS Appl. Energy Mater.* **2020**, *3*, 9.
- [89] T. Krauskopf, C. Pompe, M. A. Kraft, W. G. Zeier, *Chem. Mater.* **2017**, *29*, 8859.
- [90] W. Arnold, D. A. Buchberger, Y. Li, M. Sunkara, T. Druffel, H. Wang, *J. Power Sources*

**2020**, *464*, 228158.

- [91] X. Feng, H. Fang, P. Liu, N. Wu, E. Self, L. Yin, P. Wang, X Li, P. Jena, J. Nanda, D. Mitlin, *Angew. Chem., Int. Ed.* **2021**, *60*, 26158.
- [92] Z. Xu, X. Chen, R. Chen, X. Li, H. Zhu, *npj Comput. Mater.* **2020**, *6*, 47.
- [93] M. K. Tufail, L. Zhou, N. Ahmad, R. Chen, M. Faheem, L. Yang, W. Yang, *Chem. Eng. J.* **2021**, *407*, 127149.
- [94] B. W. Taklu, W. Su, Y. Nikodimos, K. Lakshmanan, N. T. Temesgen, P. Lin, S. Jiang, C. Huang, D. Wang, H. Sheu, S. Wu, B. J. Hwang, *Nano Energy* **2021**, *90*, 106542.
- [92] W. D. Richards, T. Tsujimura, L. J. Miara, Y. Wang, J. C. Kim, S. P. Ong, I. Uechi, N. Suzuki, G. Ceder, *Nat. Commun.* **2016**, *7*, 11009.
- [96] F. Hussain, P. Li, Z. Li, J. Yang, *Adv. Theory Simul.* **2019**, *2*, 1800138.
- [97] X. Lü, J. W. Howard, A. Chen, J. Zhu, S. Li, G. Wu, P. Dowden, H. Xu, Y. Zhao, Q. Jia, *Adv. Sci.* **2016**, *3*, 1500359.
- [98] M. Brinek, C. Hiebl, K. Hogrefe, I. Hanghofer, H. M. R. Wilkening, *J. Phys. Chem. C* **2020**, *124*, 22934.
- [99] R. Metselaar, G. Oversluizen, *J. Solid State Chem.* **1984**, *55*, 320.
- [100] A. Yelon, B. Movaghfar, H. M. Branz, *Phys. Rev. B* **1992**, *46*, 12244.
- [101] D. Di Stefano, A. Miglio, K. Robeyns, Y. Filinchuk, M. Lechartier, A. Senyshyn, H. Ishida, S. Spannenberger, D. Prutsch, S. Lunghammer, D. Rettenwander, M. Wilkening, B. Roling, Y. Kato, G. Hautier, *Chem* **2019**, *5*, 2450.
- [102] R. Chen, Z. Xu, Y. Lin, B. Lv, S. Bo, H. Zhu, *ACS Appl. Energy Mater.* **2021**, *4*, 2107.
- [103] M. Brinek, C. Hiebl, H. M. R. Wilkening, *Chem. Mater.* **2020**, *32*, 4754.
- [104] X. Feng, P. Chien, Y. Wang, S. Patel, P. Wang, H. Liu, M. Immediato-Scuotto, Y. Hu, *Energy Stor. Mater.* **2020**, *30*, 67.
- [105] Q. Zhang, W. Arnold, Z. D. Hood, Y. Li, R. Dewees, M. Chi, Z. Chen, Y. Chen, H. Wang, *ACS Appl. Energy Mater.* **2021**, *4*, 7674.

- [106] A. E. Maughan, Y. Ha, R. T. Pekarek, M. C. Schulze, *Chem. Mater.* **2021**, *33*, 5127.
- [107] Y. Yan, W. Dononelli, M. Jørgensen, J. B. Grinderslev, Y. Lee, Y. W. Cho, R. Černy', B. Hammer, T. R. Jensen, *Phys.Chem.Chem.Phys.* **2020**, *22*, 9204.
- [108] R. Theberg, A. Lund, *Solid State Ionics* **1996**, *90*, 209.
- [109] Z. Zhang, H. Li, K. Kaup, L. Zhou, P. Roy, L. F. Nazar, *Matter* **2020**, *2*, 1667.
- [110] J. G. Smith, D. J. Siegel, *Nat. Commun.* **2020**, *11*, 1483.
- [111] Z. Zhang, P. Roy, H. Li, M. Avdeev, L. F. Nazar, *J. Am. Chem. Soc.* **2019**, *141*, 19360.
- [112] L. Shen, L. Wang, Z. Wang, C. Jin, L. Peng, X. Pan, J. Sun, R. Yang, *Solid State Ionics* **2019**, *339*, 114992.
- [113] K. Homma, M. Yonemura, T. Kobayashi, M. Nagao, M. Hirayama, R Kanno, *Solid State Ionics* **2011**, *182*, 53.
- [114] K. Cao, Q. Ma, F. Tietz, B. B. Xu, M. Yan, Y. Jiang, *Sci. Bull.* **2021**, *66*, 179.
- [115] M. Balaish, J. C. G. Rosillo, K. J. Kim, Y. Zhu, Z. D. Hood, J. L. M. Rupp, *Nat. Energy* **2021**, *6*, 227.
- [116] K. Cao, X. Zhao, J. Chen, B.B. Xu, M.W. Shahzad, W.P. Sun, H.G. Pan, M. Yan, Y. Jiang, *Adv. Energy Mater.* **2022**, *12*, 2102579.

## Figures

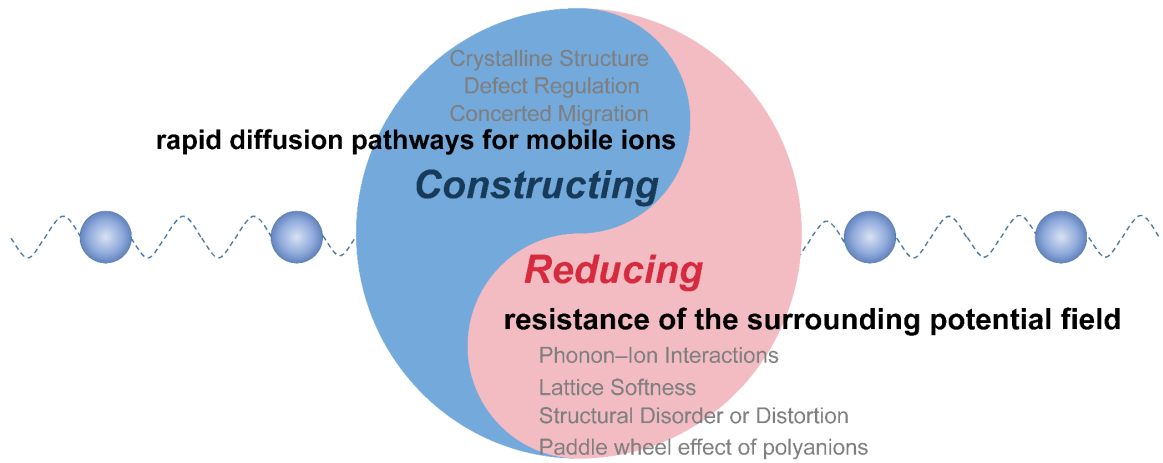


**Figure 1.** The strategies to improve ionic conductivity for solid electrolytes.

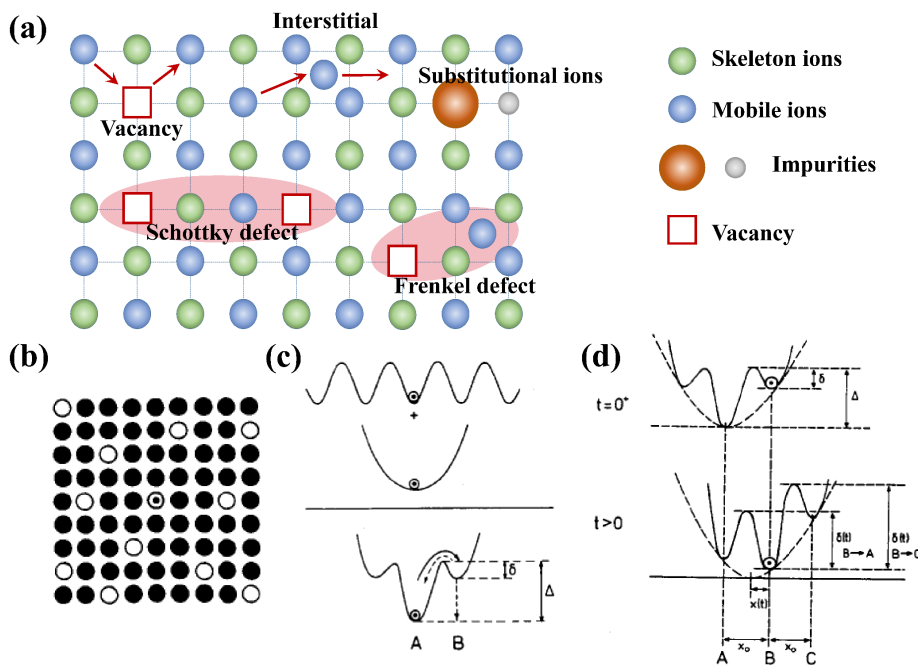


**Figure 2.** a) Schematic diagram of various point defects. b) Mobile ions (hollow circles) on a sublattice. Due to the Coulomb interaction, they tend to stay at some distance from each other. Each of them feels a Coulomb-cage potential and is expected by its neighbors to be at the position of its cage-effect minimum.<sup>[32]</sup> Copyright 1993, Elsevier. c) The single particle

potential. Superposition of the periodic lattice potential provided by the skeleton ions and of the cage-effect potential yields the single-particle potential actually experienced by the ion.<sup>[32]</sup>

Copyright 1993, Elsevier. d) Development of the potential with time after a hop.<sup>[32]</sup> Copyright 1993, Elsevier.

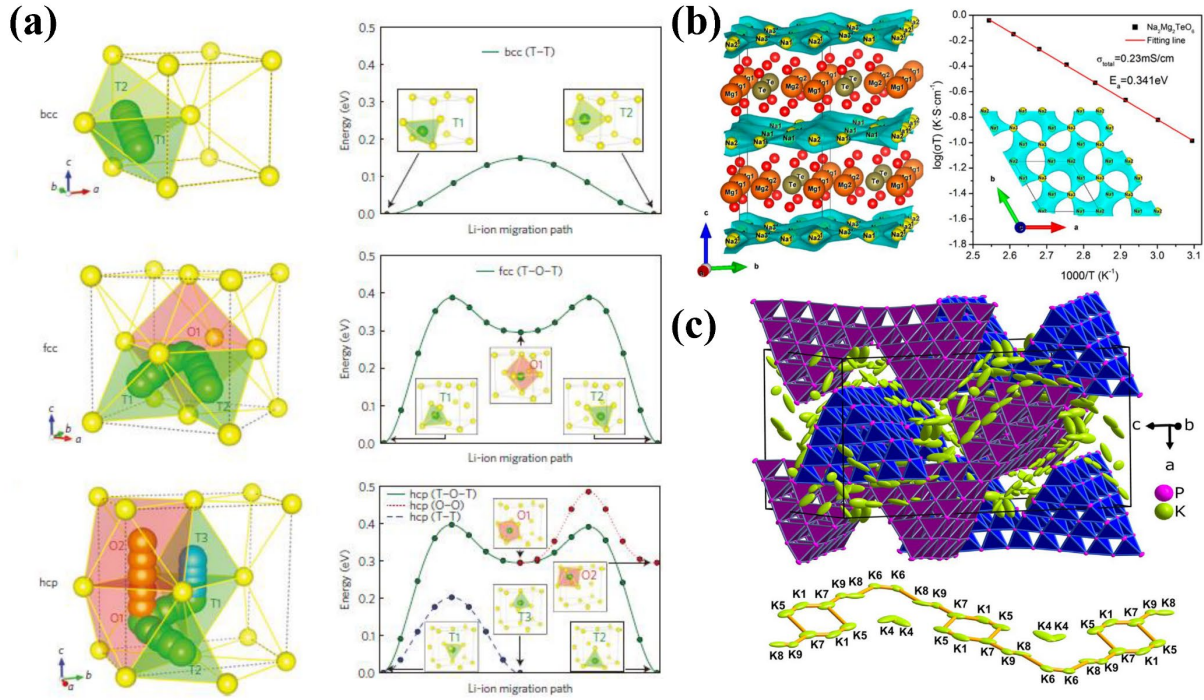


**Figure 3.** a) Li-ion migration pathways in bcc/fcc/hcp-type anion lattices.<sup>[37]</sup> Copyright 2015, Springer Nature. b) Three-dimensional bond valence difference map isosurfaces for Na<sub>2</sub>Mg<sub>2</sub>TeO<sub>6</sub>.<sup>[39]</sup> Copyright 2018, American Chemical Society. c) Unit cell of KSi<sub>2</sub>P<sub>3</sub> with large displacements of the K ions and K positions in the voids along [111] indicating a possible ion migration pathway.<sup>[40]</sup> Copyright 2021, Wiley-VCH.

**Table 1.** Representative materials and structures of solid electrolytes for various active ions.

Active Ion	Materials	Structure	Ionic Conductivity (S cm <sup>-1</sup> )	Ref.
Li <sup>+</sup>	Li <sub>3x</sub> La <sub>2/3-x</sub> TiO <sub>3</sub>	Perovskite	10 <sup>-3</sup>	[45]
	Li <sub>3</sub> OCl	Perovskite	10 <sup>-3</sup>	[46]
	Li <sub>7</sub> La <sub>3</sub> Zr <sub>2</sub> O <sub>12</sub>	Garnet	10 <sup>-4</sup> ~ 10 <sup>-3</sup>	[47]
	Li <sub>7</sub> P <sub>3</sub> S <sub>11</sub>	LISICON	10 <sup>-3</sup> ~ 10 <sup>-2</sup>	[48]
	Li <sub>10</sub> GeP <sub>2</sub> S <sub>12</sub>	LISICON	10 <sup>-2</sup>	[49]
	Li <sub>1.3</sub> Al <sub>0.3</sub> Ti <sub>1.7</sub> (PO <sub>4</sub> ) <sub>3</sub>	NaSICON	10 <sup>-3</sup>	[50]
Na <sup>+</sup>	β-Al <sub>2</sub> O <sub>3</sub>	P63/mmc	~1 (at 300°C)	[51]
	Na <sub>3</sub> Zr <sub>2</sub> Si <sub>2</sub> PO <sub>12</sub>	NaSICON	10 <sup>-3</sup>	[52]
	Na <sub>3</sub> PS <sub>4</sub>	cubic, tetragonal, glass	10 <sup>-4</sup> ~ 10 <sup>-3</sup>	[53]
K <sup>+</sup>	K <sub>1-2x</sub> Pb <sub>x</sub> GaO <sub>2</sub>	—	10 <sup>-3</sup> (at 300°C)	[54]
	K <sub>2-2x</sub> Al <sub>2-x</sub> P <sub>x</sub> O <sub>4</sub>	—	10 <sup>-3</sup> (at 200°C)	[55]

	KSi <sub>2</sub> P <sub>3</sub>	—	10 <sup>-4</sup>	[40]
Mg <sup>2+</sup>	MgSc <sub>2</sub> Se <sub>4</sub>	—	10 <sup>-4</sup>	[28]
Ca <sup>2+</sup>	Ca <sub>0.5</sub> Zr <sub>2</sub> (PO <sub>4</sub> ) <sub>3</sub>	NaSICON	10 <sup>-5</sup> (at 600°C)	[56]
Al <sup>3+</sup>	Al <sub>2</sub> (WO <sub>4</sub> ) <sub>3</sub>	—	10 <sup>-5</sup> (at 800°C)	[57]

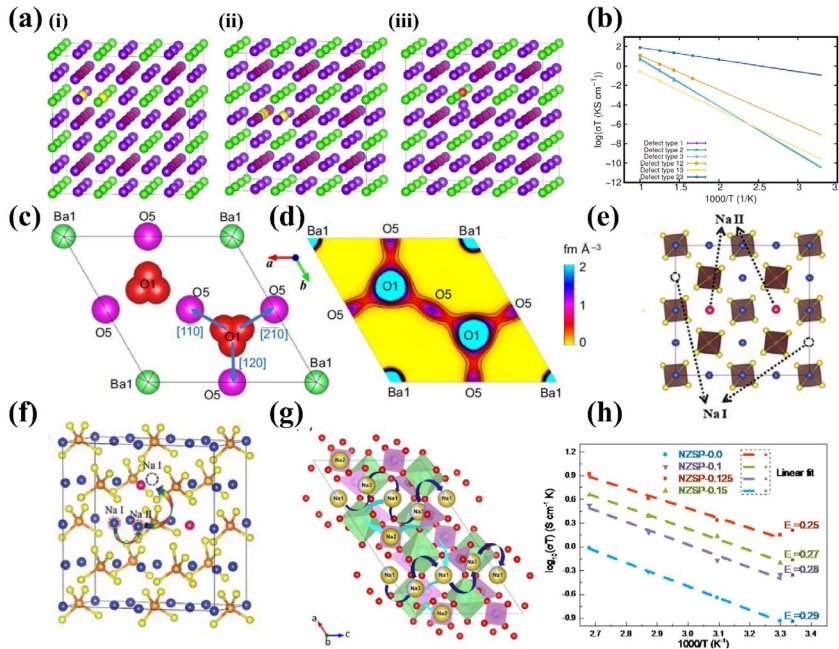


**Figure 4.** a) Structures of Li<sub>3</sub>OCl with various defects: (i) LiCl Schottky defect, Li<sub>3-x</sub>OCl<sub>1-x</sub>, denoted by defect type 1, (ii) Li<sub>2</sub>O Schottky defect, Li<sub>3-2x</sub>O<sub>1-x</sub>Cl, denoted by defect type 2, (iii) O-Cl substitution, Li<sub>3+x</sub>O<sub>1+x</sub>Cl<sub>1-x</sub>, denoted by defect type 3.<sup>[59]</sup> Copyright 2021, Elsevier. b) Arrhenius plot of the Nernst–Einstein conductivity multiplied by the temperature for defective Li<sub>3</sub>OCl samples with uniform distributions of defects.<sup>[59]</sup> Copyright 2021, Elsevier. c) Refined crystal structure on the ab plane at z=0 of Ba<sub>7</sub>Nb<sub>3.9</sub>Mo<sub>1.1</sub>O<sub>20.05</sub> at 800 °C. Arrows denote the directions of oxide-ion O1-to-O5 migration.<sup>[60]</sup> Copyright 2021, Springer Nature. d) Corresponding maximum-entropy method neutron scattering length densities (MEM NSLDs) distribution.<sup>[60]</sup> Copyright 2021, Springer Nature. e) Supercell crystal structures of t-Ca<sub>x</sub>Na<sub>3-x</sub>PS<sub>4</sub>.<sup>[63]</sup> Copyright 2020, Royal Society of Chemistry. f) Na ion migration pathways for t-Ca<sub>0.25</sub>Na<sub>2.5</sub>PS<sub>4</sub>.<sup>[63]</sup> Copyright 2020, Royal Society of Chemistry. g) The crystalline structure and migration pathways of NaSICON.<sup>[64]</sup> Copyright 2021, Elsevier. h) Arrhenius plots of the conductivity of NaSICON samples (NZSP-0.0, NZSP-0.1, NZSP-0.125, NZSP-0.15) with linear fits. The activation energies E<sub>a</sub> are indicated as 0.25, 0.27, 0.28, and 0.29 eV.

conductivity as a function of the temperature for  $\text{Na}_{3+x}\text{Zr}_{2-x}\text{Sc}_x\text{Ge}_x(\text{SiO}_4)_2(\text{PO}_4)$ .<sup>[64]</sup> Copyright 2021, Elsevier.

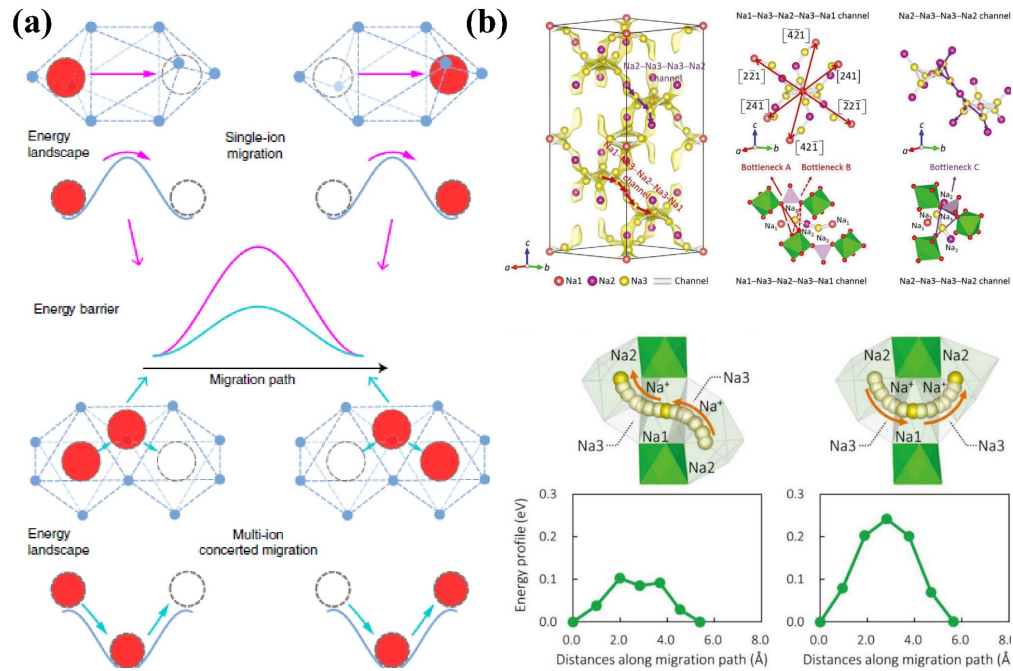


**Figure 5.** a) Schematic illustration of single-ion migration versus multi-ion concerted migration. For single-ion migration (upper insets), the migration energy barrier is the same as the barrier of the energy landscape. In contrast, the concerted migration of multiple ions (lower insets) has a lower energy barrier as a result of strong ion-ion interactions and unique mobile ion configuration in super-ionic conductors.<sup>[69]</sup> Copyright 2017, Springer Nature. b)  $\text{Na}^+$  ion migration channels and three  $\text{Na}^+$  sites of rhombohedral  $\text{NaZr}_2(\text{PO}_4)_3$  obtained from crystal structure analysis and BVEL method. The energy landscape of two  $\text{Na}^+$  ions concerted migration along the same direction (left panel) and the different directions (right panel) is shown in lower insets.<sup>[70]</sup> Copyright 2020, Wiley-VCH.

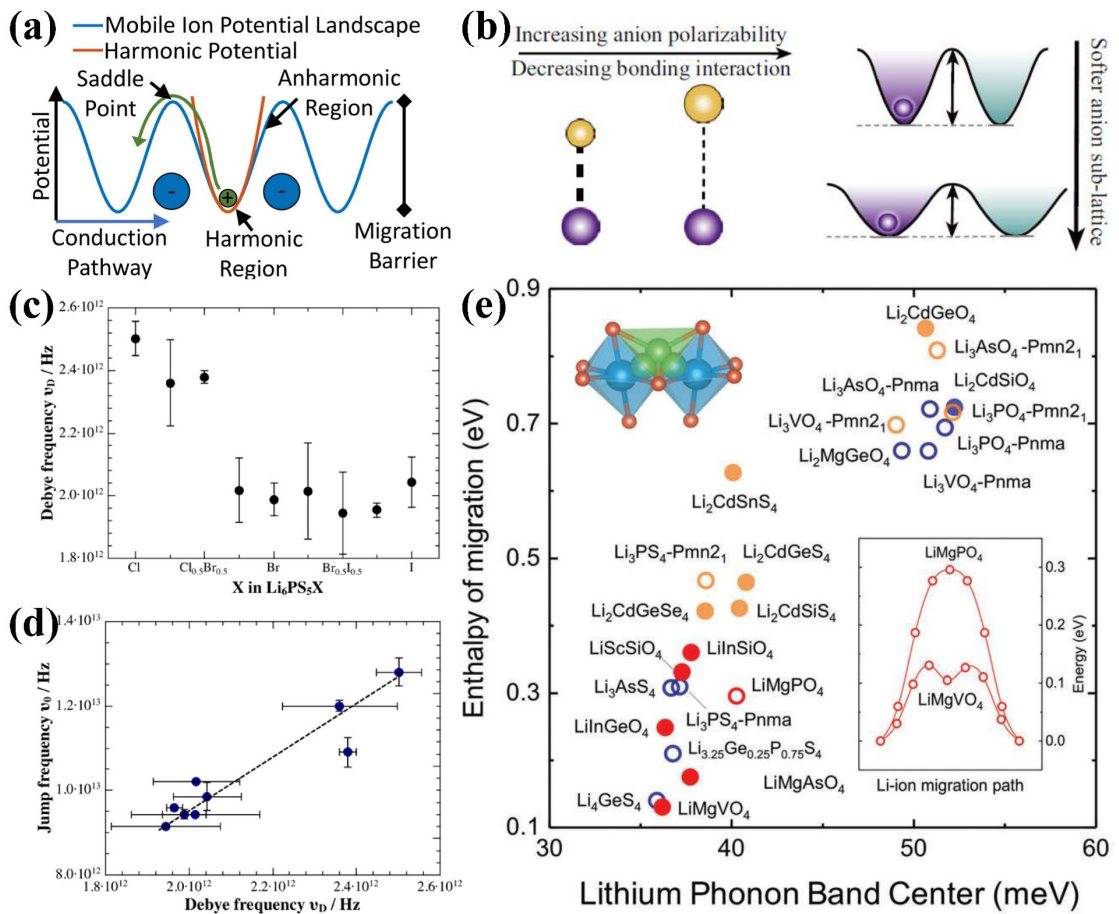


**Figure 6.** a) Conventional ion transport mechanism: A mobile ion (green circle) hops (green arrow) across barriers in the potential landscape due to the host lattice (blue circles) and surrounding mobile ions.<sup>[80]</sup> Copyright 2020, American Physical Society. b) Schematic for a mobile species and corresponding energy landscape. Increasing polarizability of the anions leads to longer and weaker bonds that soften the anion sublattice, which in turn affects the energy landscape.<sup>[76]</sup> Copyright 2021, Wiley-VCH. c) Debye frequencies in the series of  $\text{Li}_6\text{PS}_5\text{X}$  solid solutions. With increasing polarizability of the halide anion, the Debye frequency decreases.<sup>[83]</sup> Copyright 2017, American Chemical Society. d) Jump frequencies as obtained from the measured activation barriers and crystallographic jump distances against the obtained Debye frequencies.<sup>[83]</sup> Copyright 2017, American Chemical Society. e) Correlation between computed Li-phonon band center and the computed enthalpy of migration for Li-ion conductors.<sup>[75]</sup> Copyright 2018, The Royal Society of Chemistry

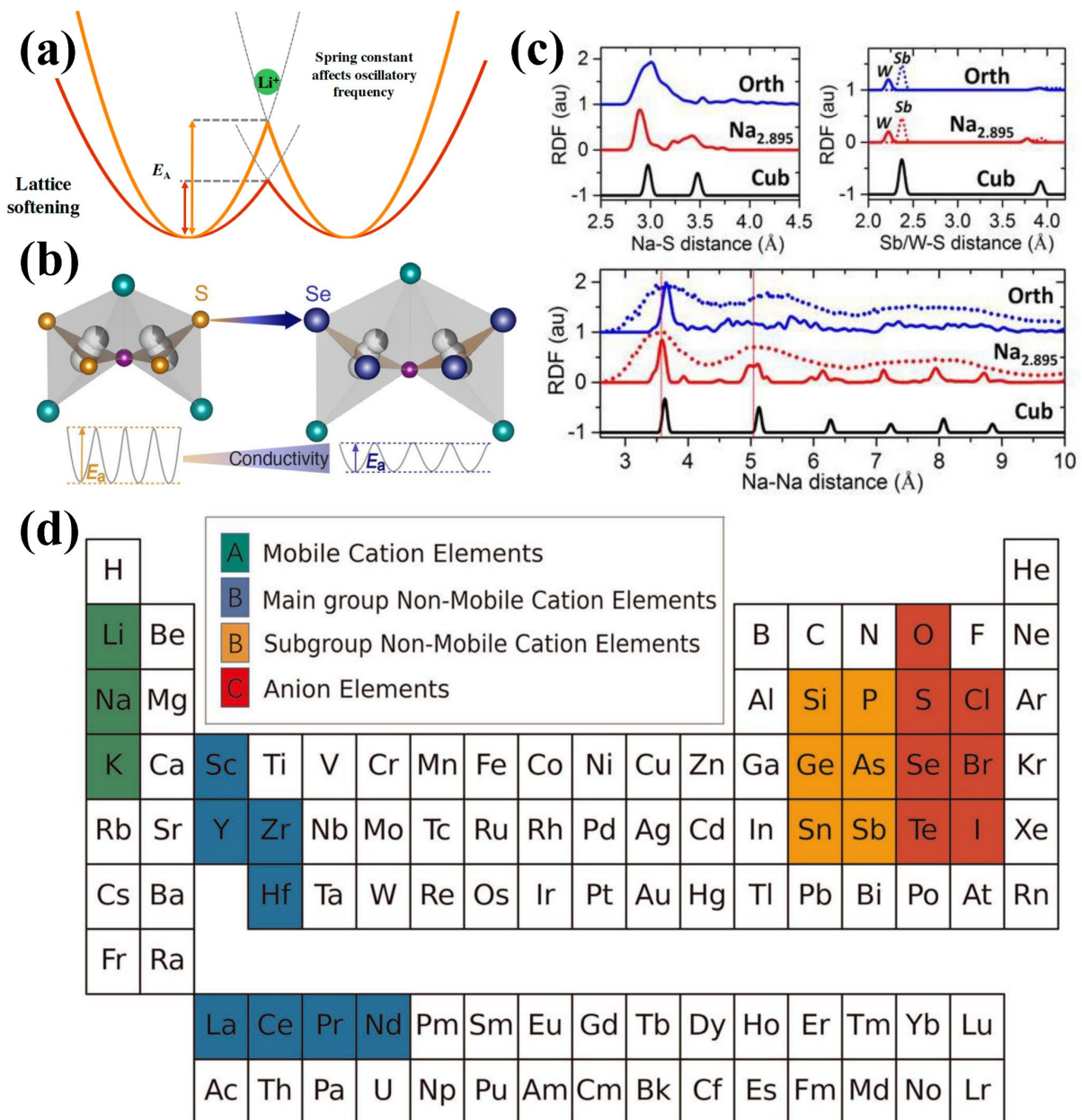


**Figure 7.** a) Schematic of the effect of lattice softening on the ion jump.<sup>[83]</sup> Copyright 2017, American Chemical Society. b) The influence of isoelectronic substitution of sulfur with selenium in  $\text{Li}_6\text{PS}_{5-x}\text{Se}_x\text{I}$ .<sup>[88]</sup> Copyright 2020, American Chemical Society. c) Calculated Na-S, Sb/W-S and Na-Na radial distribution functions (RDF) for the orthorhombic  $\text{Na}_{2.7}\text{W}_{0.3}\text{Sb}_{0.7}\text{S}_4$  (Orth) and pseudo-cubic  $\text{Na}_{2.895}\text{W}_{0.3}\text{Sb}_{0.7}\text{S}_4$  ( $\text{Na}_{2.895}$ ), compared to those of the cubic phase of  $\text{Na}_3\text{SbS}_4$  (Cub) which exhibits the exceptionally low activation energy.<sup>[91]</sup> Copyright 2021, Wiley-VCH. d) The recommended element choices for ABC ternary ionic conductors in the periodic table of element.<sup>[92]</sup> Copyright 2020, Springer Nature.

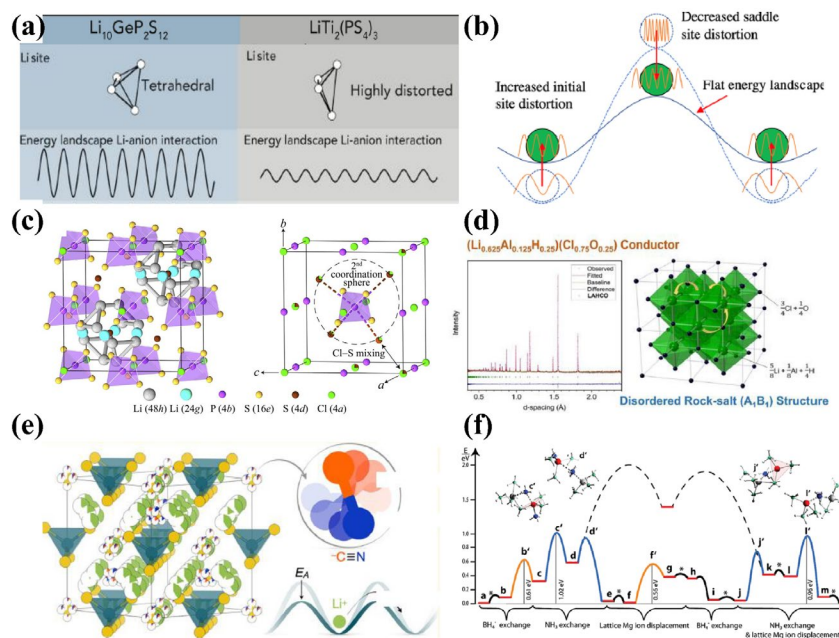


**Figure 8.** a) Schematic of the difference of  $\text{Li}_{10}\text{GeP}_2\text{S}_{12}$  and  $\text{LiTi}_2(\text{PS}_4)_3$ .<sup>[101]</sup> Copyright 2019, Elsevier. b) Schematic of the effect of distorted structure.<sup>[102]</sup> Copyright 2021, American Chemical Society. c) Crystal structure of cubic  $\text{Li}_6\text{PS}_5\text{Cl}$  with ordered packing of Cl (Wyckoff 4a) and S (Wyckoff 4d) and site disorder induced by S/Cl.<sup>[104]</sup> Copyright 2020, Elsevier. d) Neutron diffraction patterns along with Rietveld refinement and proposed average crystal structure of the pure phase LAHCO, with the formula of  $(\text{Li}_{0.625}\text{Al}_{0.125}\text{H}_{0.25})(\text{Cl}_{0.75}\text{O}_{0.25})$ .<sup>[105]</sup> Copyright 2021, American Chemical Society. e) Crystal structure of the cyanide argyrodite  $\text{Li}_6\text{PS}_5\text{CN}$  with orientationally disordered cyanide ions.<sup>[106]</sup> Copyright 2021, American Chemical Society. f) Energy profile of an interstitial magnesium ion migrating along the b-axis through the unit cell of  $\text{Mg}(\text{BH}_4)_2\text{NH}_3$  obtained by first-principles calculations.<sup>[107]</sup> Copyright 2020, The Royal Society of Chemistry.

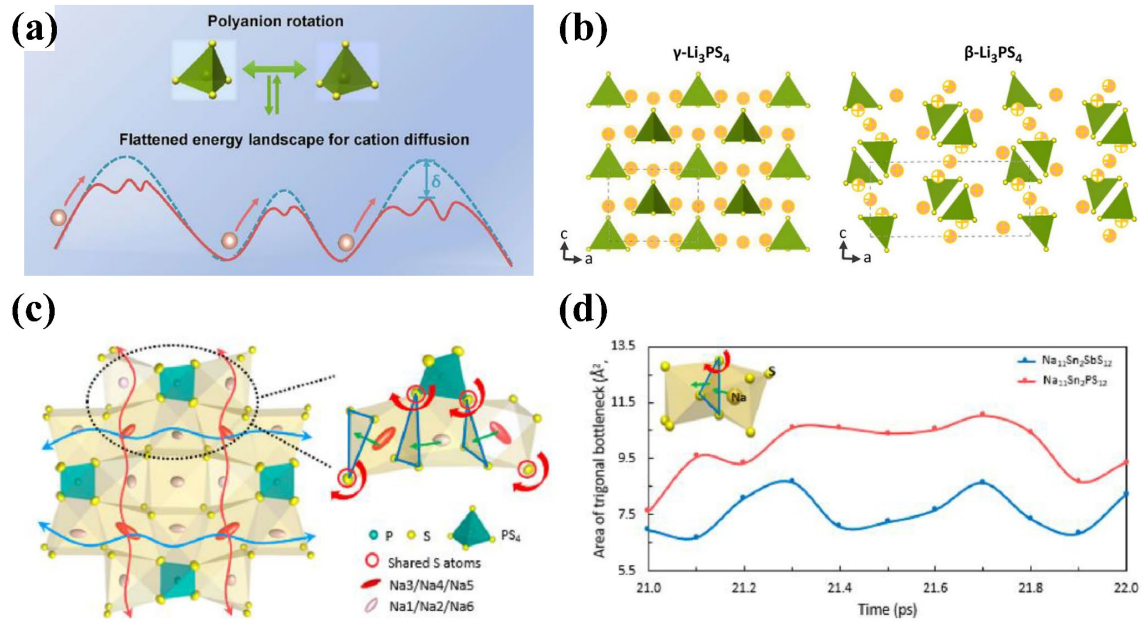


**Figure 9.** a) Schematic of the paddle wheel effect and the variational energy landscape.<sup>[109]</sup> Copyright 2020, Elsevier. b) Arrangement of the  $[\text{PS}_4]$  polyanion in  $\gamma\text{-Li}_3\text{PS}_4$  and  $\beta\text{-Li}_3\text{PS}_4$ .<sup>[109]</sup> Copyright 2020, Elsevier. c) The schematic plot of the influence of the polyanions on the trigonal bottleneck that the  $\text{Na}^+$  hop through; the red solid circles indicate the S atoms shared by the  $[\text{PS}_4]$  tetrahedron and  $[\text{NaS}_6]$  octahedron.<sup>[111]</sup> Copyright 2019, American Chemical Society. d) The area of the trigonal bottleneck for  $\text{Na}^+$  transport in both  $\text{Na}_{11}\text{Sn}_2\text{PS}_{12}$  and  $[\text{Na}_{11}\text{Sn}_2]\text{SbS}_{12}$ ; widening of the bottleneck size is evidenced when the shared S atom rotates in  $[\text{Na}_{11}\text{Sn}_2]\text{PS}_{12}$ .<sup>[111]</sup> Copyright 2019, American Chemical Society.

**Table 2.** Typical applications of various strategies and the enhanced performance.

Strategy	Material	Active ion	Specific measure	enhanced ionic conductivity ( $\text{S cm}^{-1}$ )	reduced activation energy (eV)	Ref.
Defect Regulation	$\text{Li}_{6.5}\text{Ga}_{0.2}\text{La}_{2.9}\text{Sr}_{0.1}\text{Zr}_2\text{O}_{12}$	$\text{Li}^+$	Ga, Sr co-doping	$3.03 \times 10^{-5} \rightarrow 5.50 \times 10^{-4}$	0.31	112
	$\text{Na}_{3.125}\text{Zr}_{1.75}\text{Sc}_{0.125}\text{Ge}_{0.125}\text{Si}_{2\text{PO}}_{12}$	$\text{Na}^+$	Sc, Ge co-doping	$3.9 \times 10^{-4} \rightarrow 4.64 \times 10^{-3}$	0.25	64
	$\text{Ba}_7\text{Nb}_{3.9}\text{Mo}_{1.1}\text{O}_{20.05}$	$\text{O}^{2-}$	introduced in synthesis process	$5.8 \times 10^{-4}$	$0.51 \sim 0.35 \rightarrow 0.21$	60
	c-Ca <sub>0.125</sub> Na <sub>2.75</sub> PS <sub>4</sub> t-Ca <sub>0.25</sub> Na <sub>2.5</sub> PS <sub>4</sub>	$\text{Na}^+$	Ca doping	not reported	$0.24 \rightarrow 0.17^*$ $0.21 \rightarrow 0.19^*$	63
Concerted Migration	$\text{Li}_{6.75}\text{Sb}_{0.25}\text{Si}_{0.75}\text{S}_5\text{I}$	$\text{Li}^+$	Si doping	$3 \times 10^{-6} \rightarrow 1.31 \times 10^{-2}$	$0.32 \rightarrow 0.17$	71
	LiAlSO	$\text{Li}^+$	Theoretically predicted	not reported	0.05*	67
	$\text{Ba}_{0.6}\text{La}_{0.4}\text{F}_{2.4}$	$\text{F}^-$	Substitution of $\text{La}^{3+}$ for $\text{Ba}^{2+}$	$10^{-9} \rightarrow 10^{-4}$	not reported	68
	$\text{Li}_x\text{Ag}_{1-x}\text{CrS}_2$	$\text{Li}^+$	adding Li	$2.73 \times 10^{-5} \rightarrow 1.96 \times 10^{-2}$	$0.47 \rightarrow 0.18^*$	74
Lattice Softness	$\text{Li}_3\text{ErI}_6$	$\text{Li}^+$	Substitution of I for $\text{Cl}^-$	$6.5 \times 10^{-4}$	0.37	87
	$\text{Li}_6\text{PS}_{5-x}\text{Se}_x\text{I}$	$\text{Li}^+$	Substitution of $\text{Se}^{2-}$ for $\text{S}^{2-}$	$2.5 \times 10^{-6} \rightarrow 2.8 \times 10^{-4}$	$0.38 \rightarrow 0.28^*$	88
	$\text{Na}_3\text{PS}_{4-x}\text{Se}_x$	$\text{Na}^+$	Substitution of $\text{Se}^{2-}$ for $\text{S}^{2-}$	$10^{-5} \rightarrow 10^{-4}$	$0.38 \rightarrow 0.25^*$	89
	$\text{Na}_{2.895}\text{W}_{0.3}\text{Sb}_{0.7}\text{S}_4$	$\text{Na}^+$	W-doped $\text{Na}_3\text{SbS}_4$	$2 \times 10^{-4} \rightarrow 2.42 \times 10^{-2}$	$0.28 \rightarrow 0.09$	91
Structural Disorder or Distortion	$\text{Li}_7\text{Sb}_{0.05}\text{P}_{2.95}\text{S}_{10.5}\text{I}_{0.5}$	$\text{Li}^+$	Sb, I co-doping	$1.4 \times 10^{-3} \rightarrow 2.55 \times 10^{-3}$	not reported	93
	$\text{LiTi}_2(\text{PS}_4)_3$	$\text{Li}^+$	Highly distorted Li site	$6.1 \times 10^{-3}$	0.277	101
	$\text{Li}_6\text{PS}_5\text{I}$	$\text{Li}^+$	structural disorder by soft mechanical treatment	$1 \times 10^{-6} \rightarrow 5 \times 10^{-4}$	$0.47 \rightarrow 0.36$	103
	$\text{Li}_{6-x}\text{PS}_{5-x}\text{Cl}_{1+x}$	$\text{Li}^+$	Cl/S disorder	$2 \times 10^{-6} \rightarrow 1.9 \times 10^{-2}$	$0.5 \rightarrow 0.22$	104
Paddle Wheel Mechanism of Polyanions	$\text{Li}_{0.625}\text{Al}_{0.125}\text{H}_{0.25}\text{Cl}_{0.75}\text{O}_{0.25}$	$\text{Li}^+$	Li/Al/H and Cl/O site disorder	$10^{-7} \rightarrow 10^{-4}$	0.41	105
	$\text{Li}_6\text{PS}_5\text{CN}$	$\text{Li}^+$	(-CN) disorder	$6 \times 10^{-5}$	0.47	106
	$\text{Mg}(\text{BH}_4)_2\text{NH}_3$	$\text{Mg}^{2+}$	highly flexible structure	$10^{-11} \rightarrow 3.3 \times 10^{-4}$	$2 \rightarrow 0.96$	107
	$\beta\text{-Li}_3\text{PS}_4$	$\text{Li}^+$	Rotation of $[\text{PS}_4]$ tetrahedron	$3 \times 10^{-7}$ (RT) $\rightarrow 3 \times 10^{-2}$ (500K)	not reported	113
Mechanism of Polyanions	$\text{Li}_{3.25}\text{Si}_{0.25}\text{P}_{0.75}\text{S}_4$	$\text{Li}^+$	Rotation of $[\text{PS}_4]/[\text{SiS}_4]$	$10^{-7} \rightarrow 1.2 \times 10^{-3}$	$0.35 \rightarrow 0.30^*$	109
	$\text{Na}_{11}\text{Sn}_2\text{PnX}_{12}$ (Pn = P, Sb; X = S, Se).	$\text{Na}^+$	Rotation of $[\text{PnX}_4]^{3-}$ anion	not reported	$0.15 \sim 0.21^*$	111

\*) Theoretical data, RT) Room temperature



**Caiyun Wang** received her Bachelor degree in Material Science and Engineering from Zhejiang University in 2018. She is currently a Ph.D. candidate under the supervision of Prof. Jiang in Zhejiang University. Her research interests focus mainly on solid electrolyte energy materials and electrochemistry for rechargeable metal ion batteries.



**Ben Bin Xu** is a professor of materials and mechanics in the Department of Mechanical and Construction Engineering at Northumbria University, UK. He obtained his Ph.D. in Mechanical Engineering (2011) at Heriot-Watt University in Edinburgh. He then moved to the University of Massachusetts, Amherst, USA, to work (2011-2013) with Prof. Ryan C. Hayward as a postdoc. His research interests include materials chemistry, responsive materials, soft matter physics, mechanics, and micro-engineering.



**Xuan Zhang** received his doctorate in the Department of Materials Engineering at KU Leuven in 2018. After completion of PhD, he was working as a postdoctoral fellow at the same institute. He obtained his BSc and MSc degrees in Physical Chemistry from Lanzhou University in China. He has published over 45 peer-reviewed journal papers. His current research focuses on MOFs films and electrode materials for separation, sensors, catalysis and energy storage and conversion devices.



**Wenping Sun** is professor at School of Materials Science and Engineering, Zhejiang University. He received his B.S. in 2008 and Ph.D. in materials science in 2013 from the University of Science and Technology of China (USTC). His research expertise includes electrocatalysis, fuel cells, and batteries, especially the design of novel materials and structures, and fundamental understanding of related electrochemical processes.



**Jian Chen** is a Professor of Institute of Science and Technology for New Energy, Xi'an Technological University, China. He received his PhD from Northwestern Polytechnical University, China. His current research interests focus on the development and application of energy storage and conversion materials including battery materials, hydrogen storage materials, and electrocatalyst, and high entropy alloys.



**Hongge Pan** received his PhD in Materials Science and Engineering from Zhejiang University in 1996 under a joint program between Zhejiang University and Institute of Physics, Chinese Academy of Science. Later that year he joined Zhejiang University and became a Professor in 1999. His research is focused on energy materials for solid-state hydrogen storage and lithium batteries.



**Mi Yan** received his Ph.D. in Department of Mechanical Engineering from Southeast University, China in 1991. He joined Zhejiang University as a lecturer in 1991 and became a Professor in 1998. His research is focused on magnetic materials and energy materials.



**Yinzhu Jiang** is a professor at School of Materials Science and Engineering in Zhejiang University, China. He received his Ph.D. degree in Department of Materials Science and Engineering from University of Science and Technology of China in 2007. He worked as a post-doctoral researcher in Heriot-Watt University, United Kingdom from 2007 to 2008 and an Alexander von Humboldt Fellow in Bielefeld University, Germany from 2008 to 2010. His research interests focus mainly on energy-related materials and electrochemistry, including rechargeable batteries, metal anodes and solid electrolytes.

A comprehensive discussion and the-state-of-art summary of strategies for enhancing ionic conductivity for inorganic solid electrolytes are provided from the basic mechanism of ion hopping. The elaboration of two main principles: constructing rapid diffusion pathways and reducing resistance of the surrounding potential field establish the scientific basic toward designing and searching extraordinary materials for next generation battery systems.

*Caiyun Wang, Ben Bin Xu, Xuan Zhang, Wenping Sun, Jian Chen, Hongge Pan, Mi Yan, Yinzhu Jiang\**

## **Ion Hopping: Design Principles for Strategies to Improve Ionic Conductivity for Inorganic Solid Electrolytes**

